NASA Contractor Report 172392

Development of Improved Low-Strain Creep Strength in CABOT® alloy No. R-41 Sheet

M. F. Rothman

Cabot Corporation
1020 W. Park Avenue
Kokomo, IN 46901

NASA

National Aeronautics and
Space Administration

Langley Research Center
Hampton, Virginia 23665

Development of Improved Low-Strain Creep Strength in CABOT® alloy No. R-41 Sheet

M. F. Rothman

Cabot Corporation
1020 W. Park Avenue
Kokomo, IN 46901

N84-31346#

Table of Contents

Table of Contents (Cont.)

SUMMARY

The purpose of this investigation was to improve the low strain ($\leq$ 1 percent) creep strength of CABOT® alloy No. R-41, thin-gauge sheet by means of optimized thermomechanical processing treatment. Two major approaches were undertaken in an effort to achieve this objective. The first was to evaluate new heat treatments designed to provide a coarse grain structure without severely reducing the tensile ductility. The other was to determine if the development of a preferred crystallographic annealing texture in the sheet would improve the creep strength.

To assist in the performance of the program, Cabot Corporation established baseline data for sheet product manufactured in the laboratory from standard production, hot-rolled plate using the same procedures as normally employed in full-scale production of such product. All experimental work was performed utilizing the exact same piece of hot-rolled plate feedstock. The baseline data generated included tensile properties from room temperature to 1365 K (2000°F), low strain creep strength in the temperature range of 920 K (1200°F) to 1255 K (1800°F), and stress rupture strength in the range of 1035 K (1400°F) to 1255 K (1800°F).

Significant improvements in low strain creep strength were achieved at temperatures greater than 1090 K (1500°F) with newly developed heat treatments. The more ambitious of the two heat treatments developed, involving a solution treatment temperature of 1475 K (2200°F), produced a coarse grain structure (ASTM 2 to 3) with attendant increased higher temperature creep and stress rupture properties compared with the baseline material (ASTM 6 to 7). This heat treatment provides for an upward shift in a plot of creep strength versus the Larson-Miller parameter of as much as $\Delta P_K = 1,100$ ($\Delta P_R = 2,000$) parameter units in the vicinity of 1255 K (1800°F).

The improved creep properties developed with this first new heat treatment are accompanied by values for tensile ductility at temperatures of 1035 K (1400°F) or above which are equivalent to or better than those produced with the standard baseline heat treatment. At temperatures below 1035 K (1400°F), the tensile ductility is reduced, but not below acceptable engineering levels for this class of material. Tensile yield strength obtained with this heat treatment is substantially lower than that for the baseline material.

The second new heat treatment developed, which involves a less ambitious solution treatment temperature of 1420 K (2100°F), produces a grain size of ASTM 4 to 5 and an upward shift in creep strength in terms of the Larson-Miller parameter value at a given stress of about $\Delta P_K = 350$ to 365 ($\Delta P_R = 630$ to 660) parameter units at temperatures near 1255 K (1800°F). The advantage or disadvantage accruing at lower temperatures was not determined. Tensile properties, at least at 1145 K

® CABOT is a registered trademark of Cabot Corporation.

(1600°F), do not appear to be adversely affected by this treatment.

All attempts to produce an improvement in low strain creep strength of the study alloy by generating a preferred crystallographic annealing texture in the final sheet product were unsuccessful. This may be a consequence of the fact that the maximum strength texture component areas shown in a stereographic projection pole figure were all less than three times the random intensity and thus not really indicative of a pronounced texture. Or, it may simply be that alloys of the type being studied do not lend themselves to strengthening by texture development.

1.0 INTRODUCTION

This investigation was undertaken to determine if the low-strain (< 1 percent) creep strength of CABOT alloy No. R-41, thin-gauge sheet could be increased through modification of thermomechanical processing procedures. The application for such an optimized form of material would be in the construction of heat shields for advanced re-entry vehicles.

Recent studies indicate creep may be a significant factor in the design of heat shields for reusable thermal protection systems for advanced re-entry and/or hypersonic vehicles. Optimization of heat shields for maximum reuse with minimum weight requires the use of thin-sheet materials with thicknesses of 1 mm or less. Because of heat shield deflection limit criteria, the area of interest for heat shield design encompasses low ranges of creep strain where the details of material behavior are least understood (ref. 1).

CABOT alloy No. R-41, a nickel-base sheet alloy developed by the General Electric Company, has shown promise for these heat shield applications. Like most alloys, however, lower strengths than normal result when the material is utilized in thin gauge form. From the data of Greene (ref. 2) and others (ref. 3-5), it appears that the creep strength of alloy No. R-41 is not a function of sheet thickness in the range from about 1.0 mm (0.040-inch) to 2.0 mm (0.080-inch); however, in the range from 0.13 mm (0.005-inch) to 0.5 mm (0.020-inch), Greene (ref. 2) indicates generally lower creep properties, though the data are not extensive.

In order to facilitate the comparison of the properties derived for an optimized alloy No. R-41 material to the capabilities of normal alloy No. R-41 sheet product, Cabot Corporation undertook the development of limited baseline creep, stress rupture, and tensile data for standard material nominally 0.64 mm (0.025-inch) in thickness. This included tensile properties from room temperature to 1365 K (2000°F), 0.5 percent and 1.0 percent creep properties in the temperature range from 920 K (1200°F) to 1255 K (1800°F), and stress rupture properties in the temperature range from 1035 K (1400°F) to 1255 K (1800°F). These data were generated for material derived from a single production heat of alloy No. R-41. They do not reflect the normal variation in properties to be expected as a function of considering several heats, which usually accrues as a result of chemistry differences and minor processing differences.

The experimental and baseline property programs were performed using sheet produced in the laboratory from standard production, hot-rolled, plate feedstock. All creep and tensile testing was performed by a single in-house testing group to prevent the introduction of lab-to-lab testing variation effects. The stress rupture tests were performed using two different laboratories, but care was taken to supervise the conduct of the testing so as to avoid variations in testing procedures.

Improvements in the low-strain creep properties of alloy No. R-41 were sought using two different approaches. One was to examine the

development of an optimized heat treatment to provide a coarse grain structure without a concomitant deleterious effect upon the tensile properties. The other was to determine if low strain creep properties in the study alloy could be enhanced through generation of a preferred crystallographic orientation in the cold-rolled and annealed sheet product.

In both studies, initial screening tests for creep properties were performed using 1145 K/97 MPa (1600°F/14 KSI) imposed conditions. In the case of the heat treatment study, additional screening tests were conducted at 1255 K (1800°F), with stresses of from 14 to 28 MPa (2 to 4 KSI). Extensive mechanical property evaluations were performed for selected heat treatments developed. Effects of these heat treatment variations upon the microstructure of the material were also characterized.

Certain commercial materials are identified in this report in order to specify adequately which materials were investigated in the study. In no case does this identification imply recommendation or endorsement of the product by the National Aeronautics and Space Administration.

4

2.0 CABOT BASELINE DATA

2.1 Materials

For the purpose of developing baseline data, sheet nominally 0.64 mm (0.025-inch) in thickness was produced in the laboratory by cold rolling standard-production, 4.75 mm (0.187-inch) thick, hot-rolled plate of CABOT alloy No. R-41 using the standard production rolling and annealing procedures. Only the product of a single production heat was used. All material tested was first subjected to the standard solution heat treatment and aged as specified by General Electric (ref. 6), namely, 1395 K (2050°F)/30 minutes/AC + 1170 K (1650°F)/4 hours/AC.

The chemistry of the material used, for both this baseline study and subsequent experimental work, was:

Weight Percent

Al	B	C	Co	Cr	Fe	Mo	Ni	P	S	Ti
1.48	.007	.08	11.08	18.85	3.36	10.07	Bal	.003	< .002	3.16

Microstructural characterization of the material produced was performed using optical and electron microscopy. Typical structures were observed. Results of these examinations are presented later in this report in Section 3.1-Effects of Solution Treatment Temperature.

2.2 Tensile Properties

Duplicate transverse specimens were tensile tested in air at room temperature, 920 K (1200°F), 1035 K (1400°F), 1145 K (1600°F), 1255 K (1800°F), and 1365 K (2000°F). The specimen configuration employed for these tests was the same as that illustrated in Appendix A. In addition, tabs were spot welded to the grip ends of each sample to prevent distortion from occurring around the pin holes during testing. For elevated temperature tests, a radiant furnace equipped with Quartz infrared lamps was used to maintain the test temperature within ± 3 K (± 5°F) of the desired condition. Two chromel-alumel thermocouples were wired to the center of the specimen gauge area. One was used for control of the furnace, while the other served as a means to independently monitor the sample temperature. Each specimen was allowed to soak at test temperature for at least 10 minutes prior to testing.

Specimens were strained to 0.2 percent offset yield point at a rate of 0.005 mm/mm/minute (inch/inch/minute). The test was then continued to failure at an approximate strain rate of 0.05 mm/mm/minute (inch/inch/minute), based upon a cross head speed of 2.86 mm/minute (0.11 inch/minute) and a specimen reduced section length of 57.2 mm (2.25 inches). For the determination of 0.2 percent yield strengths in room-temperature tests, strain was measured using a clip-on-type extensometer with a 25.4 mm (1 inch) gauge length. The maximum strain error of the extensometer was 0.00012 (Class B2). In elevated temperature

tests, a rigid frame extensometer of the same type as that described in Appendix A was used. Strain was measured by a linear variable differential transformer which was an integral component of the extensometer. The maximum strain error of the LVDT measuring system was 0.0001 (Class B1).

The results obtained for the tensile tests performed upon the baseline material are presented in Table 1, with strength and ductility as a function of temperature shown plotted in Figures 1 and 2, respectively. Particularly noteworthy is the tensile ductility minimum in the temperature range from 1145 to 1255 K (1600 to 1800°F), obvious from an examination of Figure 2. This ductility trough is characteristic of gamma prime-strengthened, nickel-base alloys and is a key consideration in the evaluation of modified heat treatments.

2.3 Creep Properties

All creep testing was performed using the procedure described in Appendix A. All tests were performed in the transverse direction. Results of the tests, which were conducted at various stresses over the range of temperatures from 920 K (1200°F) to 1255 K (1800°F), are presented in Table 2.

In order to characterize the creep strength of the baseline sheet over the range of test conditions, the 0.5 percent and 1.0 percent creep strain data were subjected to a least squares optimization of the Larson-Miller parameter equation in the following form (ref. 7):

$$P = T(20.0 + \log t) = C_1 + C_2 \log S + C_3 (\log S)^2$$

where, P = Larson-Miller parameter
T = Absolute temperature (K or °R)
t = Time to given creep strain (hours)
S = Imposed stress (MPa or KSI)
C_1, C_2, C_3 = Optimized constants

Results of the analyses are presented in Table 3, while the regression line and simultaneous 95 percent confidence limits are shown plotted in Figures 3 and 4 for the 0.5 percent and 1.0 percent creep strain levels, respectively.

The excellent degree of fit is illustrated by the high figures calculated for the multiple correlation coefficients and indices of determination. The values for the standard error of the estimate, defined as:

$$\text{Std. Error} = \sqrt{\frac{\sum(P_{OBS} - P_{REG})^2}{N-3}}$$

6

Table 1

Summary of Baseline Tensile Test Data*

Test Temperature	U.T.S.		0.2% Y.S.		Elongation
	(MPa)	(KSI)	(MPa)	(KSI)	(%)
RT	1290	187	805	117	24
	1270	184	835	121	22
	1275	185	855	124	20
	1255	182	815	118	21
	1275	185	805	117	25
920 K (1200°F)	1150	167	780	113	17
	1130	164	760	110	17
1035 K (1400°F)	1035	150	765	111	15
	1055	153	780	113	16
1145 K (1600°F)	710	103	565	82	11
	675	98	550	80	12
	740	107	635	92	12
	750	109	635	92	13
1255 K (1800°F)	380	55	325	47	10
	365	53	290	42	11
	355	51	255	37	15
1365 K (2000°F)	76	11	48	7	30
	83	12	62	9	33

* All material solution heat treated at 1395 K (2050°F) for 30 minutes, air cooled, then aged at 1170 K (1650°F) for 4 hours.

7

TEMPERATURE (°F)

RT   1200   1400   1600   1800   2000

STRESS (MPa)

1200

1000

800

600

400

200

YIELD

ULTIMATE

STRESS (KSI)

180

160

140

120

100

80

60

40

20

RT   900   1000   1100   1200   1300
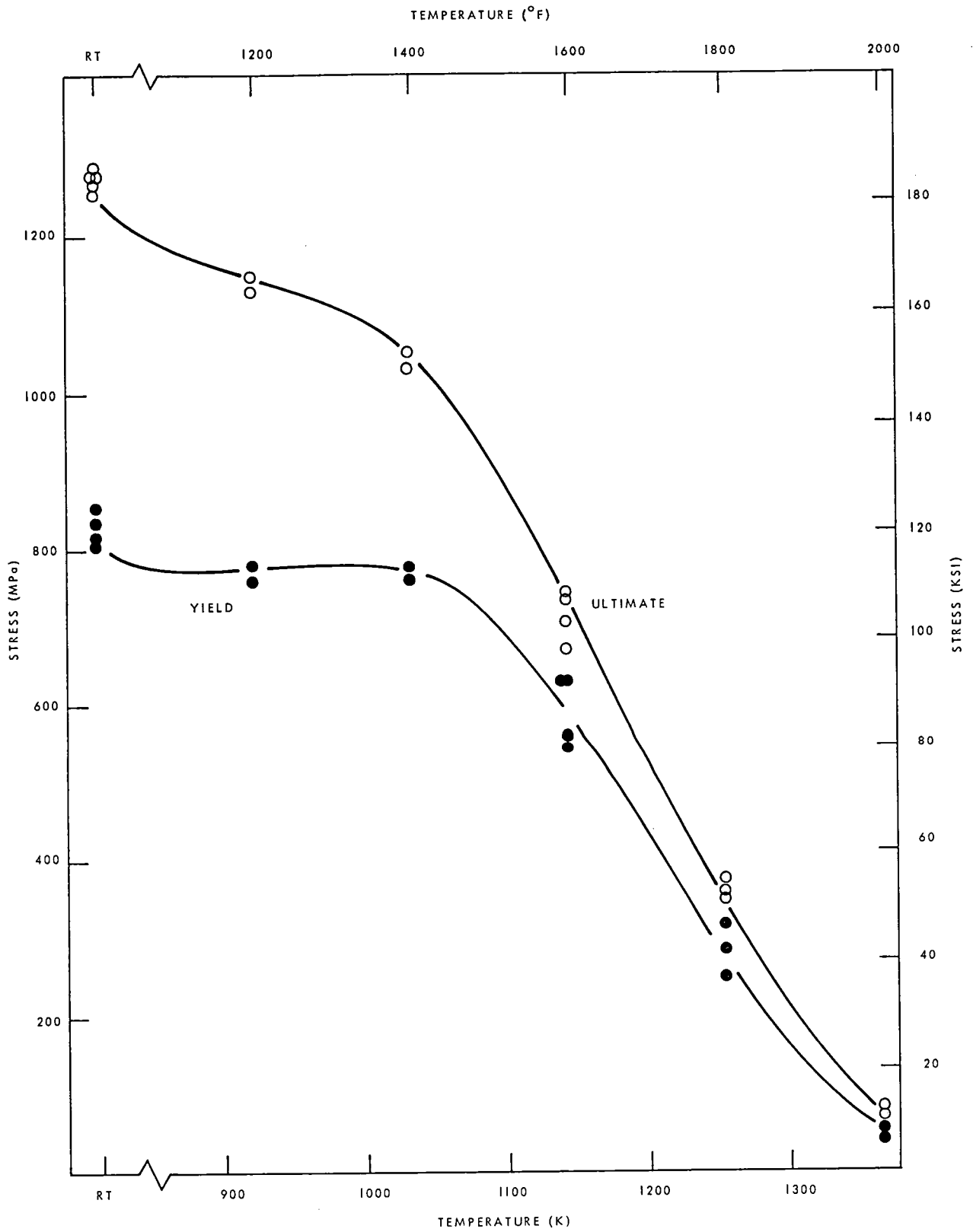
TEMPERATURE (K)

FIGURE 1:   TENSILE STRENGTH AND 0.2% OFFSET YIELD STRENGTH OF BASELINE MATERIAL AS A
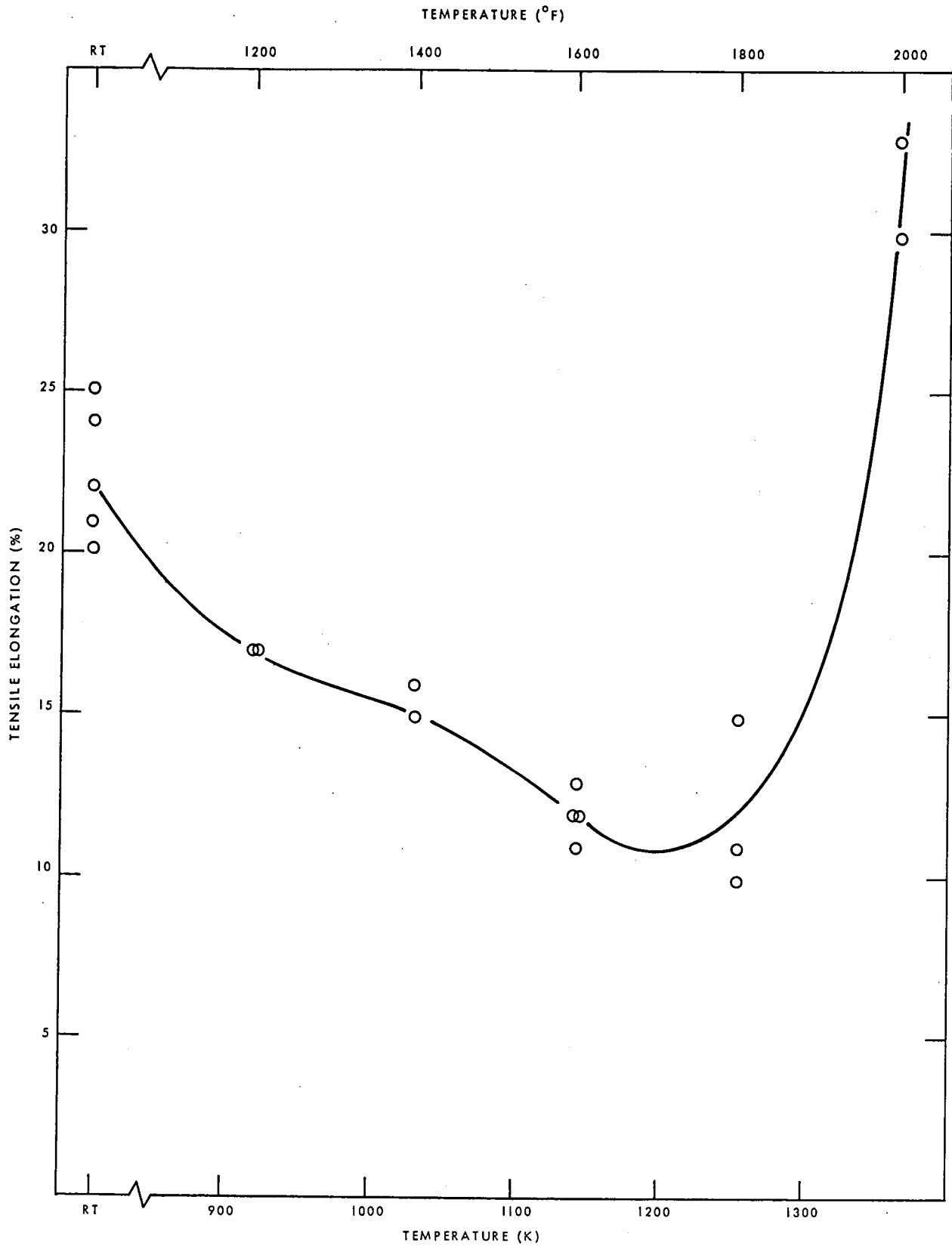   FUNCTION OF TEMPERATURE.

FIGURE 2: TENSILE ELONGATION OF BASELINE MATERIAL AS A FUNCTION OF TEMPERATURE.

9

Table 2

Summary of Baseline Creep Test Data*

Test Temperature	Test Stress (MPa)	(KSI)	Hours to % Creep 0.5%	1.0%
920 K (1200°F)	725	105	119	171
	690	100	104	158
	655	95	260	368
	620	90	440	658
	585	85	985	–
1035 K (1400°F)	470	68	5	12
	415	60	60	82
	360	52	66	98
	305	44	153	250
	250	36	242	351
1090 K (1500°F)	280	40.5	10	17
	250	36	56	86
	250	36	63	86
	215	31.5	79	123
	185	27	89	135
	155	22.5	111	203
1145 K (1600°F)	140	20	21	34
	140	20	32	50
	115	17	45	77
	97	14	56	116
	97	14	61	127
	97	14	78	154
	76	11	71	154
	55	8	655	1100
1255 K (1800°F)	21	3	14	31
	21	3	53	90
	17	2.5	43	71
	14	2	57	96
	14	2	90	142
	14	2	86	137
	10	1.5	244	395
	7	1	380	628

* All material solution heat treated at 1395 K (2050°F) for
  30 minutes, air cooled, and then aged at 1170 K (1650°F)
  for 4 hours.

Table 3

Larson-Miller Parameter Analysis for Baseline Creep Data

Regression Equation: $P = T (20.0 + \log t) = C_1 + C_2 \log S + C_3 (\log S)^2$

A. Where T = Temperature (K)
   S = Stress (MPa)
   t = Time to given creep strain (hours)

Percent Creep	Equation Constants			Std. Error of Estimate (LM Parameter Units)	Multiple Correlation Coefficient	Index of Determination
	C_1	C_2	C_3			
0.5	27,788.5	1,320.9	-1,346.9	298.9	.993	.984
1.0	27,868.2	1,624.1	-1,444.9	267.6	.994	.988

B. Where T = Temperature (°R)
   S = Stress (KSI)
   t = Time to given creep strain (hours)

Percent Creep	Equation Constants			Std. Error of Estimate (LM Parameter Units)	Multiple Correlation Coefficient	Index of Determination
	C_1	C_2	C_3			
0.5	50,308.4	-1,688.3	-2,424.4	538.0	.993	.984
1.0	50,774.7	-1,438.3	-2,600.8	481.7	.994	.988

FIGURE 3: 0.5% CREEP STRENGTH OF BASELINE MATERIAL AS A FUNCTION OF LARSON-MILLER
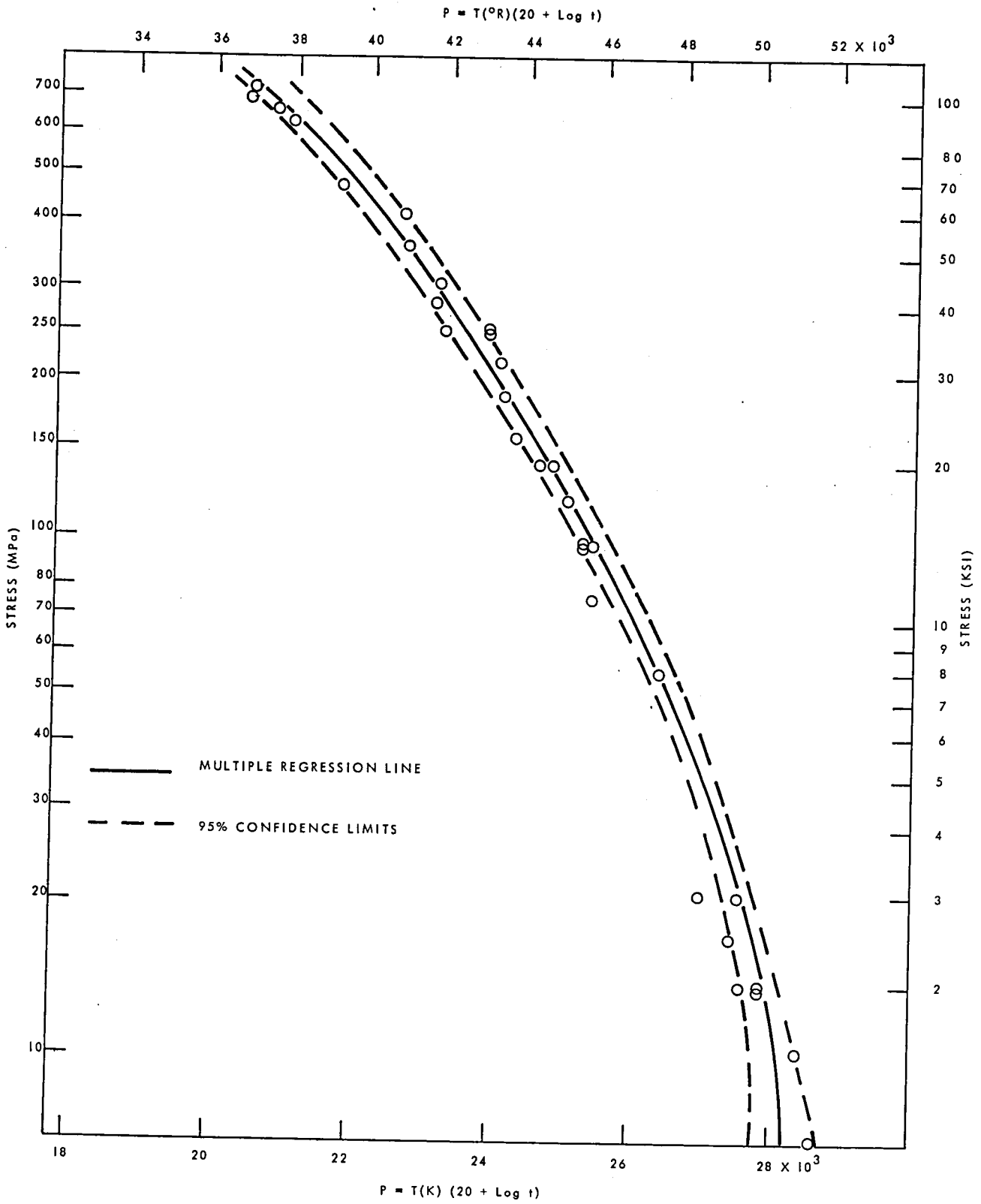   PARAMETER.

12

FIGURE 4: 1.0% CREEP STRENGTH OF BASELINE MATERIAL AS A FUNCTION OF LARSON-MILLER PARAMETER.

where, P_{OBS} = the Larson–Miller parameter calculated from the observed test results,

P_{REG} = the Larson–Miller parameter calculated from the regression analysis,

and   N   = the number of observations,

are all reasonably small, running between one and two percent of the mean value of the Larson–Miller parameters for both sets of data.

2.4 Stress Rupture Properties

Stress rupture testing was performed using transverse specimens of the same configuration as that illustrated in Appendix A. Tests were conducted at 1035 K (1400°F), 1145 K (1600°F), and 1255 K (1800°F). Results are presented in Table 4, and a plot of stress rupture strength versus the Larson–Miller parameter is given in Figure 5. In view of the limited amount of data, a statistical analysis was not performed.

14

Table 4

Summary of Baseline Stress Rupture Test Data*

Test Temperature	Test Stress (MPa)	(KSI)	Life (Hrs.)	El. (%)
1035 K (1400°F)	515	75	24	3
	515	75	20	3
	485	70	22	4
	485	70	29	7
1145 K (1600°F)	205	30	34	5
	170	25	59	4
	170	25	57	5
	170	25	56	5
1255 K (1800°F)	62	9	39	9
	62	9	35	7
	62	9	23	8

* All material solution heat treated at 1395 K (2050°F) for 30 minutes, air cooled, and then aged at 1170 K (1650°F) for 4 hours.
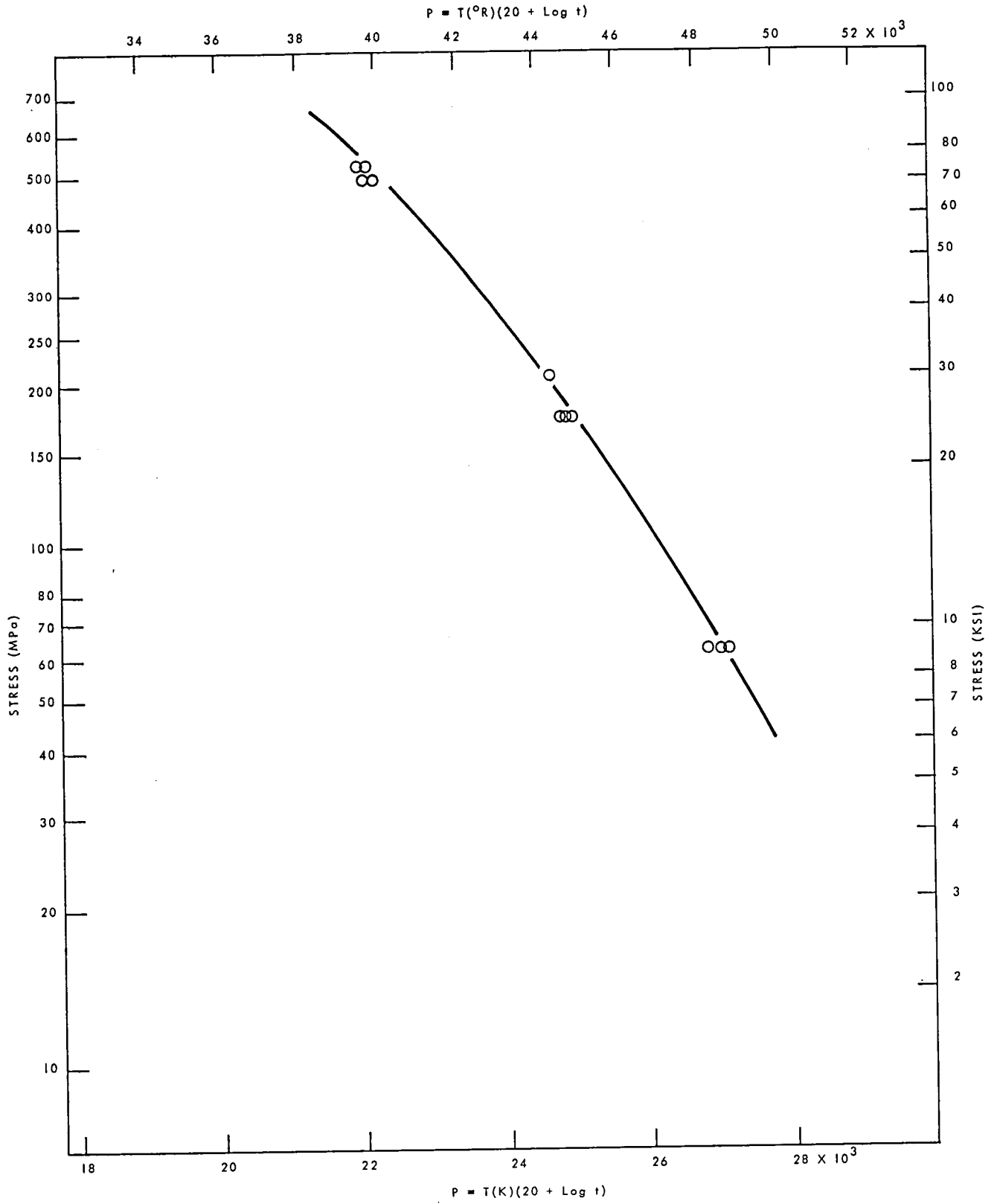
FIGURE 5: STRESS RUPTURE STRENGTH OF BASELINE MATERIAL AS A FUNCTION OF LARSON-MILLER
PARAMETER.

3.0 HEAT TREATMENT STUDY

3.1 Introduction

The effects of heat treatment upon the morphology of gamma prime and carbide phases in nickel-base superalloys and the attendant effects upon mechanical properties in the alloys are subjects that have been widely addressed in technical literature. An excellent review of the area is presented by Decker and Sims (ref. 8). It has been demonstrated by various investigators that varying the microconstituent morphology in materials like alloy No. R-41 by adjusting the heat treatment schedule can significantly alter key mechanical properties (ref. 9-19).

Two distinct heat treatment approaches for alloy No. R-41 evolved from early developmental work. A low-temperature solution treatment at typically 1340 K (1950°F) was recommended for a fine-grained, high-yield-strength, production configuration, while a high-temperature, solution treatment at typically 1450 K (2150°F) was to be used for obtaining a coarser-grained, optimized stress rupture strength product (ref. 9). In his work, Chang (ref. 9) recognized quite early that solution treating at the higher temperature caused downstream cracking problems during fabrication. He attributed this to dissolution of primary M_6C-type carbides during the solution treatment at 1450 K (2150°F) and reprecipitation of deleterious $M_{23}C_6$ carbide films during subsequent thermal treatments.

Out of this finding and other work in the early 1960's, the now commonly employed compromise solution treatment temperature of 1395 K (2050°F) arose. This provided for a larger grain size and attendant higher temperature creep and rupture strengths than that produced for the 1340 K (1950°F) solution treatment without promoting the deleterious carbide morphologies.

Although the problems presented by solution treating alloy No. R-41 at temperatures above 1395 K (2050°F) have been often reported and discussed in literature, little apparent work has been directed at developing a heat treatment approach which would allow the production of a coarse-grained material without the accompanying carbide precipitation problems and loss of tensile ductility. The work of Prager (ref. 11) comes closest to addressing this issue comprehensively, but is limited in focus to the concept of improving the tensile ductility of material with low ductility after the 1340 K (1950°F) heat treatment. It does not look to the effect upon creep properties nor the question of solution temperatures over 1450 K (2150°F).

In the present study, the influence of solution treatment temperatures up to 1475 K (2200°F) are characterized for thin gauge sheet. Major attention is devoted to post solution treatment aging techniques for material initially solution treated both above and below the M_6C solvus temperature of 1435 K (2125°F). Characterization of the initial variations in solution treatment temperature consists basically of an examination of the tensile properties from room temperature to 1255 K

(1800°F) and selected creep properties at 1145 K (1600°F) and 1255 K (1800°F). An in-depth examination of the effects of aging treatments for material solution treated at 1475 K (2200°F) was performed, and a number of treatments were selected for broad spectrum testing of tensile, creep, and stress rupture properties, the results for which are presented in the following sections.

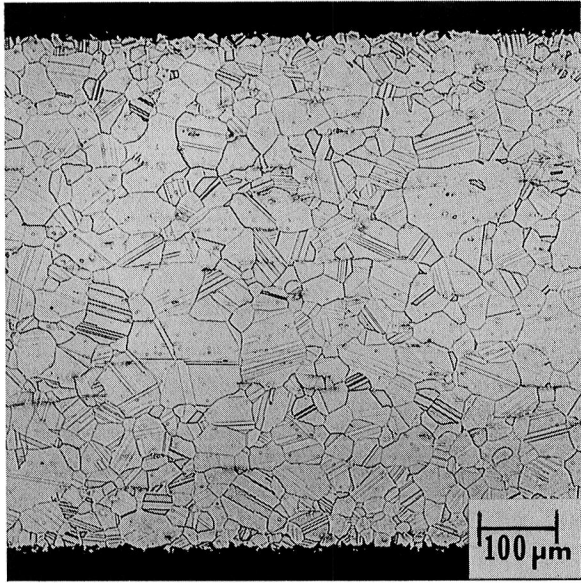### 3.2 Effect of Solution Treatment Temperature Variation with Standard Aging Treatment

Microstructures:

Samples were solution treated for 30 minutes at 1395 K (2050°F), 1420 K (2100°F), 1450 K (2150°F), and 1475 K (2200°F) and air cooled. All were then aged for four hours at 1170 K (1650°F). The influence of the solution treatment temperature upon the grain size of the material is quite graphically illustrated by the optical photomicrographs presented in Figure 6. The increase in grain size with increasing temperature may be easily discerned and is quite pronounced upon going from 1420 K (2100°F), which is below the M_6C carbide solvus temperature, to 1450 K (2150°F), which is above the M_6C solvus temperature.

Quantitative grain size measurements, arrived at by the comparison of numerous fields of view at 100X magnification to standard drawings, are presented in Table 5. The baseline 1395 K (2050°F) solution-treated material exhibits a uniform ASTM 6-7 grain size. Grain structures produced at increasingly higher solution treatment temperatures are increasingly less uniform, as well as larger on the average. The 1475 K (2200°F) solution-treated material has an average grain size of ASTM 2-3, but exhibits isolated grains as large as ASTM 0.5-1 on occasion.

Photomicrographs obtained using the electron microscope for each of the four solution treatment temperatures in combination with the standard 1170 K (1650°F)/4 hour/AC age are presented in Figure 7. The baseline 1395 K (2050°F) solution-treated material exhibits small, discrete M_6C carbides at the grain boundaries, coupled with profuse gamma prime precipitation in the matrix. The structure of the 1420 K (2100°F) solution-treated material is similar to that of the baseline material, though the volume of carbides at the grain boundaries is larger. The microstructures observed for the 1450 K (2150°F) and 1475 K (2200°F) solution-treated material, on the other hand, exhibited continuous grain boundary carbide films. The field shown for the 1450 K (2150°F) treatment exhibits wedge-like carbide protrusions into the matrix area, believed to be the initial stages of a cellular $M_{23}C_6$ carbide precipitation and growth phenomenon, while for the 1475 K (2200°F) treatment, one of the grain boundaries shown exhibits what appears to be a typical $M_{23}C_6$ cellular carbide morphology.
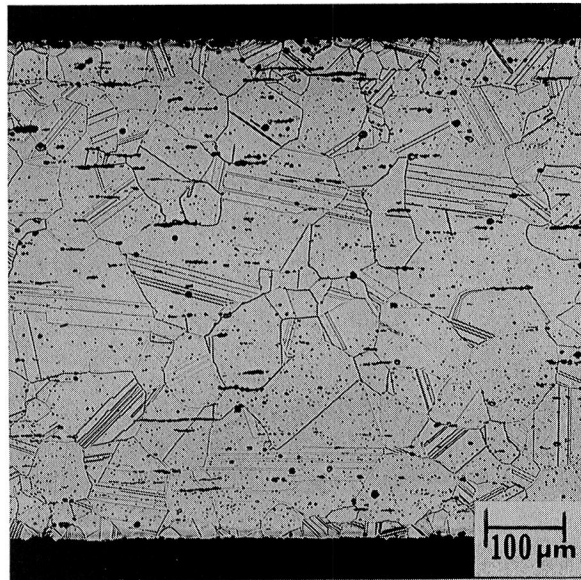
An analysis of extracted residues was performed utilizing standard x-ray diffraction techniques. Samples were ground to be 220 grit finish and cleaned with methanol. Extraction was performed using a solution of 5 percent HCl, 5 percent H_3PO_4, and 90 percent methanol and an applied

18
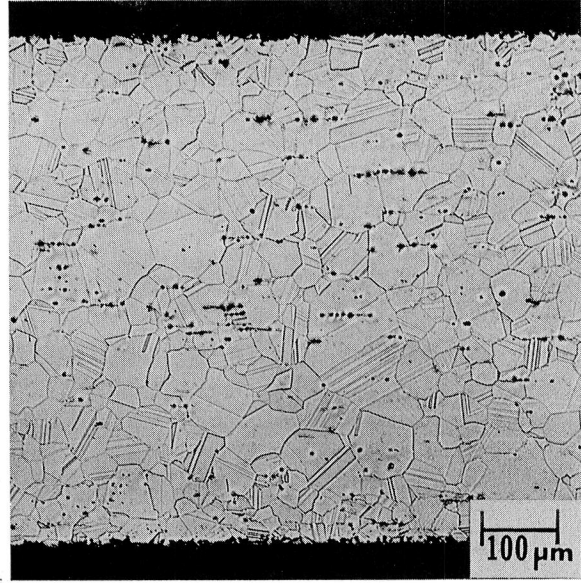
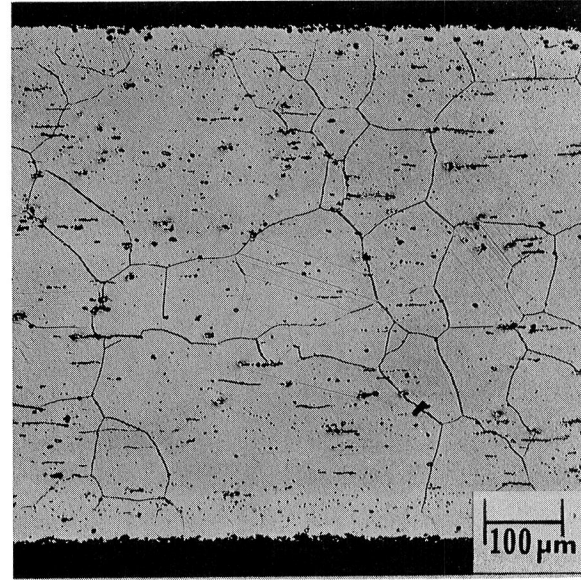(a)   (b)

(c)   (d)
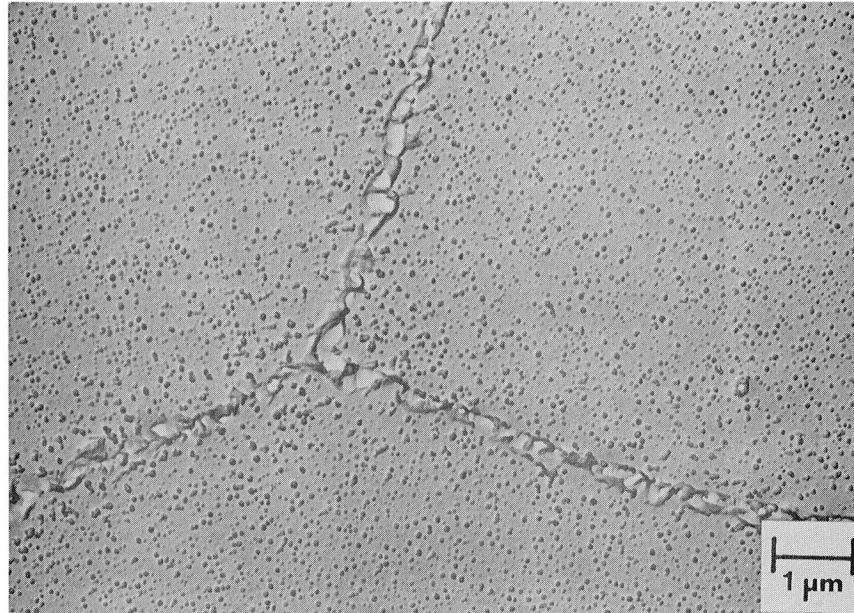
Figure 6: Effect of solution treatment temperature upon grain size.
           (a) 1395 K (2050°F); (b) 1420 K (2100°F); (c) 1450 K (2150°F);
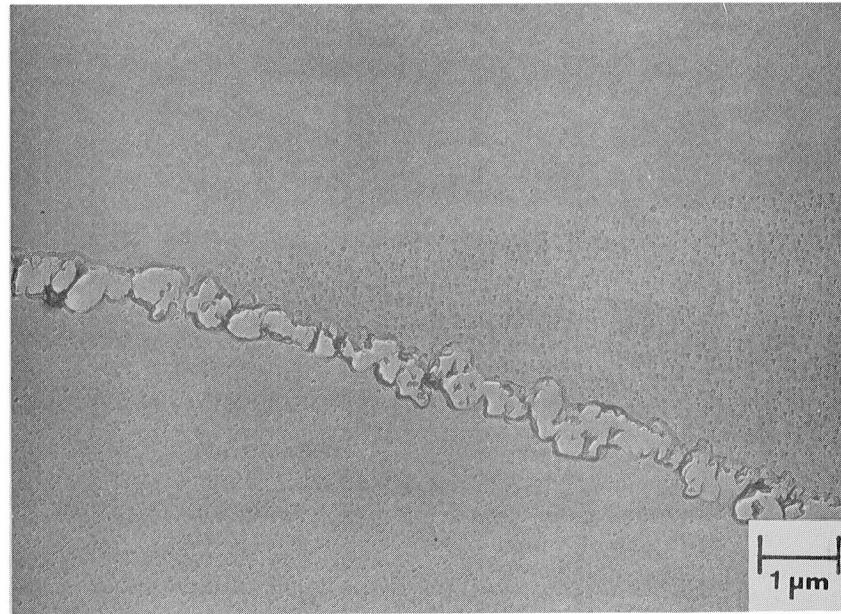   (d) 1475 K (2200°F). All 100X.

Table 5

Effect of Solution Treatment Temperature Upon Average Grain Size

Solution Treatment Temperature*	Average ASTM Grain Size
1395 K (2050°F)	6 to 7
1420 K (2100°F)	4 to 5
1450 K (2150°F)	3 to 5
1475 K (2200°F)	2 to 3

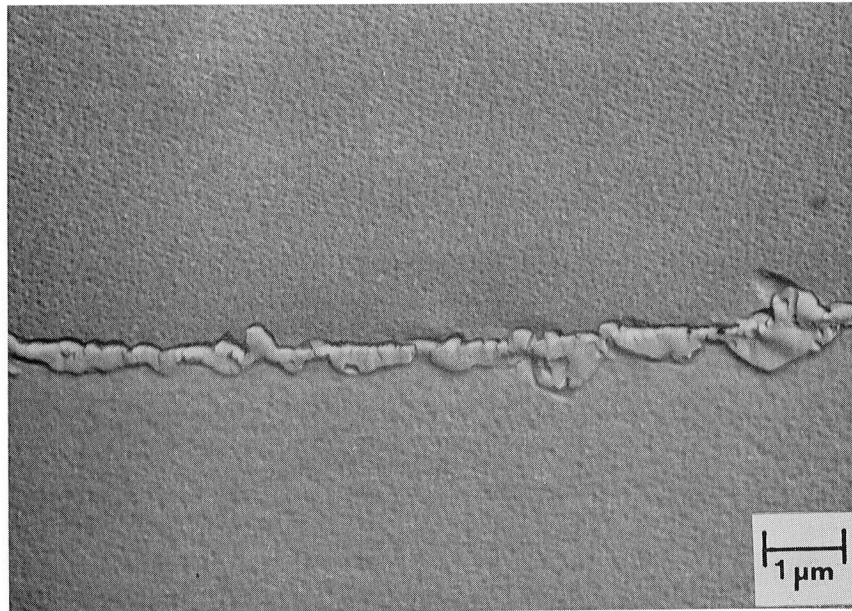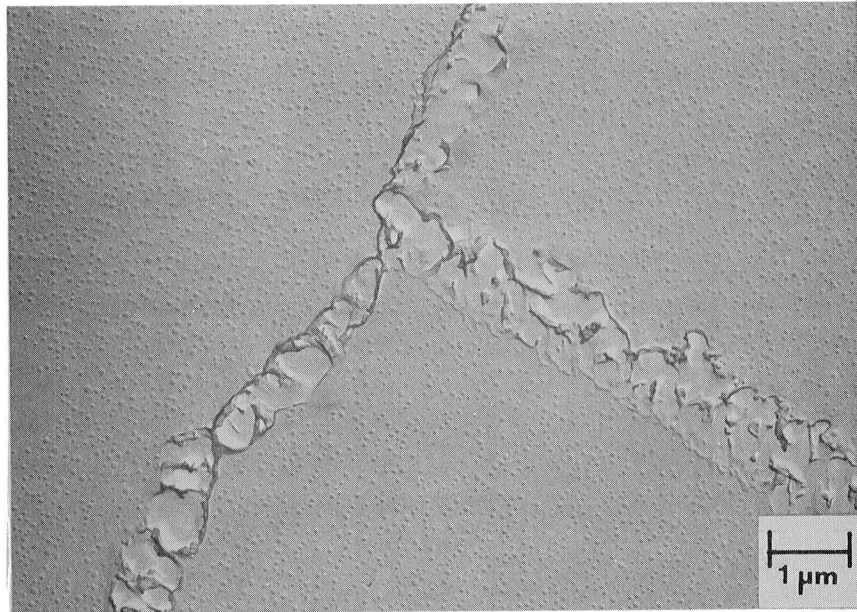* All samples received 30 minutes at temperature.

(a)

(b)

Figure 7:   Effect of solution treatment temperature upon grain boundary carbide
morphology.   (a) 1395 K (2050°F); (b) 1420 K (2100°F); (cont'd.)

(c)

(d)

Figure 7 - Concluded: (c) 1450 K (2150°F)
(d) 1475 K (2200°F). All 9400X.

22

current of 200 milliamperes for 24 hours. Residues were centrifuged, rinsed repeatedly in methanol, and dried. Debye-Scherrer x-ray photographs were taken for each of the residues utilizing a cobalt target and an iron filter. Microconstituents present in the residue were determined using the three strongest lines and relative levels measured by normalizing the various line intensities to the strength of the matrix lines.

Results of the x-ray analysis are presented in Table 6. In agreement with the results of the electron photomicrographs presented in Figure 7, the analysis indicates a general absence of $M_{23}C_6$ carbides in the samples solution treated below the M_6C solvus temperature of 1435 K (2125°F). It also indicates that $M_{23}C_6$ carbides are present for material solution treated at both 1450 K (2150°F) and 1475 K (2200°F), as suspected, with a concurrent reduction in the presence of M_6C-type carbides.

Following up on the work of Prager (ref. 11), a sample was also prepared employing a 1475 K (2200°F)/30 minute solution treatment followed by a furnace cool at approximately 55 K/hour (100°F/hour) to 1310 K (1900°F)/4 hours/AC. This treatment was designed to reprecipitate the dissolved M_6C carbides in the same globular, discrete particle morphology as produced for the solution treatments below the M_6C solvus. For the sake of comparison, a similar treatment was applied to another sample, this time omitting the furnace cool and instead involving an air cool from 1475 K (2200°F) to room temperature and a reheating to 1310 K (1900°F). Both samples were given the standard 1170 K (1650°F)/4 hours/AC age.

Typical microstructures observed for these two heat treatments using the electron microscope are shown in Figure 8 for the air cool and reheat and Figure 9 for the furnace cool. In both cases, the structures observed contain very large, discrete, presumably, M_6C carbides, with no visible evidence of $M_{23}C_6$ continuous grain boundary films.

The results for the air-cooled and reheated material contrast with the results reported by Moon et al. (ref. 13) for thicker-sectioned material, where reheating in the range of 1255 K (1800°F) to 1420 K (2100°F) following solution treating at 1450 K (2150°F) and air cooling yielded continuous grain boundary films of M_6C carbides. This may be a function of the slower heating and cooling rates experienced with massive sections. Based upon these results with thin sheet, it appeared that reheating following an air cool was as viable an approach to avoiding the deleterious carbide films as was the furnace cooling approach, and it offerred more flexibility as an industrial practice.

Creep Properties:

Duplicate and triplicate transverse creep tests were performed for material given the various solution treatments using the same specimen configuration as shown in Appendix A. Testing was performed at 1145 K (1600°F) under a stress of 97 MPa (14 KSI). Some additional tests were

Table 6

Phases Identified Using X-Ray Diffraction Analysis of Extracted Residues Taken From Samples Given Various Heat Treatments

Heat Treatment	γ'	$M_{23}C_6$	M_6C
1395 K (2050°F)/30 Minutes/AC + 1170 K (1650°F)/4 Hours/AC	S	–	S
1420 K (2100°F)/30 Minutes/AC + 1170 K (1650°F)/4 Hours/AC	S	–	S
1450 K (2150°F)/30 Minutes/AC + 1170 K (1650°F)/4 Hours/AC	S	MW	MS
1475 K (2200°F)/30 Minutes/AC + 1170 K (1650°F)/4 Hours/AC	S	MW	MS
1475 K (2200°F)/30 Minutes/AC + 1240 K (1775°F)/8 Hours/AC (D) + 1090 K (1500°F)/24 Hours/AC	S	MW	M
1475 K (2200°F)/30 Minutes/FC to 1225 K (1750°F)/4 Hours/AC (E) + 1090 K (1500°F)/24 Hours/AC	S	W	S

S – Strong Line Intensity

MS – Medium to Strong Line Intensity

M – Medium Line Intensity

MW – Medium to Weak Line Intensity
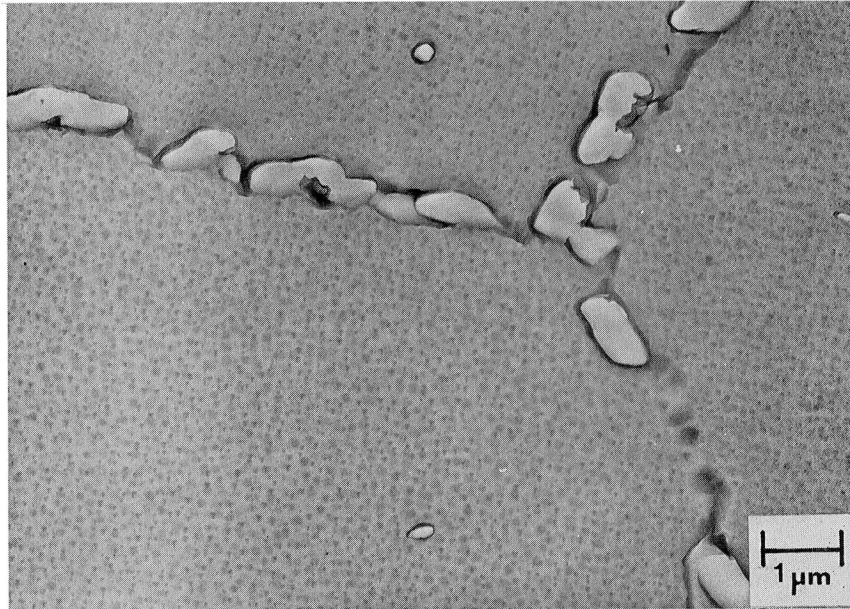
W – Weak Line Intensity

Figure 8: Microstructure following 1475 K (2200°F)/30 minute/AC +
1310 K (1900°F)/4 hour/AC + 1170 K (1650°F)/4 hour/AC
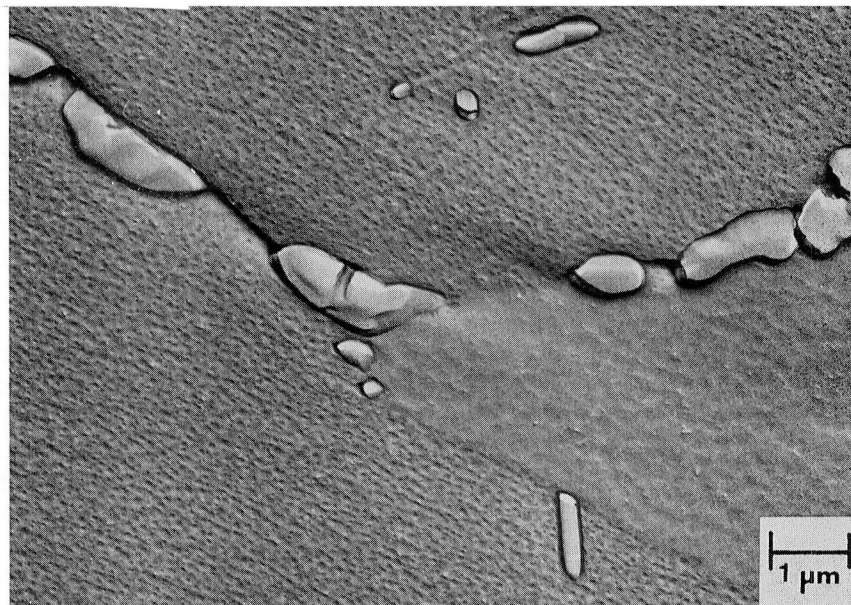heat treatment. 9400X.

Figure 9: Microstructure following 1475 K (2200°F)/30 minute/FC to
1310 K (1900°F)/4 hour/AC + 1170 K (1650°F)/4 hour/AC
heat treatment. 9400X.

25

run at 1255 K (1800°F) and 14 MPa (2 KSI). Results of the tests are reported in Table 7. The influence of the increasing grain size observed with increasing solution treatment temperature upon the low strain creep properties is quite evident at both test temperatures. This is illustrated clearly in Figure 10, which shows the 0.5 percent creep strength plotted as a function of the Larson-Miller parameter for each of the four solution treatment temperatures. The potential for increasing the low strain creep strength by increasing the grain size is appreciable, particularly at temperatures of 1255 K (1800°F).

The influence upon creep properties of interposing a furnace cool to a second solution treatment step at 1310 K (1900°F) ranged from negligible to somewhat negative, as shown in Table 7. This appeared true for initial solution treatment temperatures of both 1475 K (2200°F) and 1450 K (2150°F).

Tensile Properties:

Tensile tests were performed initially at room temperature, 1145 K (1600°F), and 1255 K (1800°F) for each of the four solution treatment temperatures in combination with the standard 1170 (1650°F)/4 hour age. Some of the tests were single tests. All were transverse and employed a specimen configuration the same as that shown in Appendix A. The test temperatures were selected on the basis of the ductility minimum exhibited by the baseline material in that range, as shown in Figure 2.

Results of these and other tests are given in Tables 8, 9, and 10 for ultimate tensile strength, 0.2 percent offset yield strength, and tensile elongation, respectively. Data are also presented for tests conducted at 920 K (1200°F) and 1035 K (1400°F) later in the program for the material solution treated at 1475 K (2200°F). These results were not available concurrent with those for 1145 K (1600°F) and 1255 K (1800°F). Consequently, the loss in tensile strength and yield strength at these lower temperatures, shown in Figures 11 and 12, respectively, was not known. More importantly, the shift in the tensile ductility minimum to 1035 K (1400°F) from 1145 K (1600°F), as shown in Figure 13, was not known.

The consequence of this was that the effect of solution treating at 1475 K (2200°F) upon yield and utlimate tensile strengths was perceived to be minimal in relation to the baseline heat treatment. Furthermore, the reduction of room-temperature tensile ductility from about 22 percent to about 10 percent was noted, but the reduction in elevated temperature ductility was not fully appreciated, as at 1145 K (1600°F) the average was still about 8-9 percent compared to about 12 percent for the baseline heat treatment. The reduction from about 15-16 percent to 4-6 percent at 1035 K (1400°F) was not known then and, therefore, 1145 K (1600°F) was erroneously selected as the key test temperature for future work on the 1475 K (2200°F) solution treatment temperature.

The effects of interposing a furnace cool to a second solution treatment step at 1310 K (1900°F) upon tensile properties of material given an initial solution treatment at either 1475 K (2200°F) or 1450 K

26

Table 7

Effect of Solution Treatment Temperature Upon
Selected Creep Properties

Hours to % Creep for Stated Test

Conditions Solution Treatment*	1145 K/97 MPa (1600°F/14 KSI)		1255 K/14 MPa (1800°F/2 KSI)	
	0.5%	1.0%	0.5%	1.0%
1395 K(2050°F)/30 Minutes/AC	56	116	57	96
	61	127	86	137
	78	154	90	142
log Av.**	64	131	76	123
1420 K(2100°F)/30 Minutes/AC	98	251	151	275
	112	307	199	425
	126	284	330	622
log Av.	111	280	215	417
1450 K(2150°F)/30 Minutes/AC	113	390	470	—
	195	620	670	—
log Av.	148	492	561	
1475 K(2200°F)/30 Minutes/AC	208	—	565	—
	250	800	2750	—
log Av.	228		1247	

Table 7 - Concluded

| Conditions | Hours to % Creep for Stated Test | | | |
| | 1145 K/97 MPa (1600°F/14 KSI) | | 1255 K/14 MPa (1800°F/2 KSI) | |
Solution Treatment	0.5%	1.0%	0.5%	1.0%
1450 K(2150°F)/30 Minutes/FC	124	268	860	–
to 1310 K(1900°F)/4 Hours/	125	327	375	985
AC	146	315		
log Av.	131	302	568	
1475 K(2200°F)/30 Minutes/FC	205	545	600	–
to 1310 K(1900°F)/4 Hours/	210	510	955	–
AC	212	583	1140	–
log Av.	209	545	868	

AC = air cooled; FC = furnace cooled.

 * = All samples aged for 4 hours at 1170 K (1650°F).
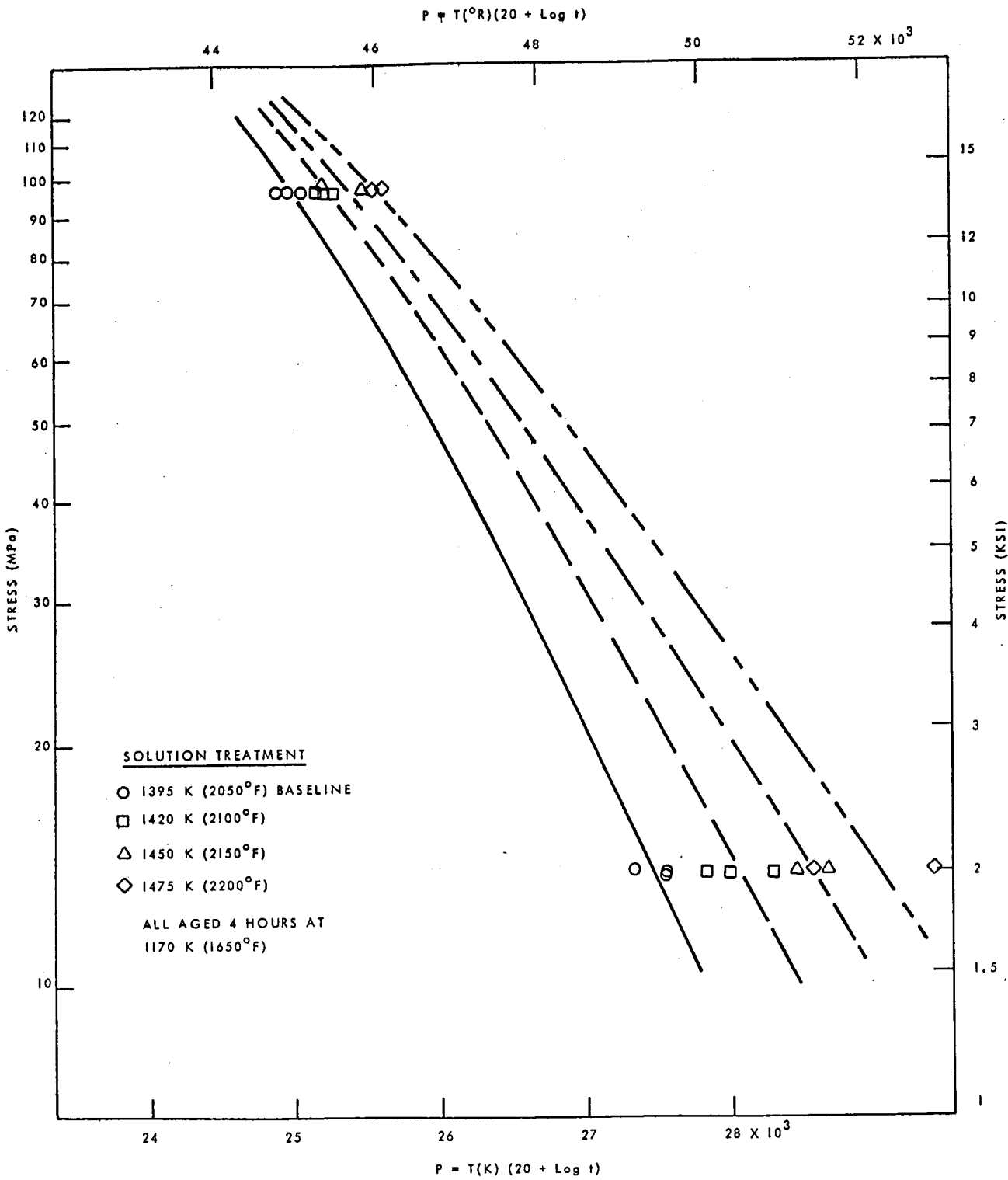** = Antilog of the average of the logarithms of the test hours.

FIGURE 10: EFFECT OF SOLUTION TREATMENT TEMPERATURE UPON 0.5% CREEP STRENGTH AS A FUNCTION OF LARSON-MILLER PARAMETER.

Table 8

Effect of Solution Treatment Temperature Upon Ultimate Tensile Strength at Various Temperatures

| Test Temperature | U.T.S. in MPa for Various Solution Treatments (30 Minutes Followed by an Air Cool)* | | | |
	1395 K (2050°F)	1420 K (2100°F)	1450 K (2150°F)	1475 K (2200°F)
Room	1290 (187) 1275 (185) 1275 (185) 1270 (184) 1255 (182)	1200 (174)	1145 (166)	1020 (148) 1005 (146) 970 (141)
920 K (1200°F)	1150 (167) 1130 (164)			820 (119) 690 (100)
1035 K (1400°F)	1055 (153) 1035 (150)			750 (109) 740 (107)
1145 K (1600°F)	750 (109) 740 (107) 710 (103) 675 (98)	745 (108) 740 (107) 725 (105) 715 (104) 670 (97)	705 (102) 690 (100)	745 (108) 730 (106) 695 (101) 685 (99)
1255 K (1800°F)	380 (55) 365 (53) 350 (51)	340 (49)	345 (50)	330 (48)

Numbers in parentheses are in KSI.
* All samples aged at 1170 K (1650°F) for 4 hours.

Table 9

Effect of Solution Treatment Temperature Upon 0.2% Tensile
Yield Strength at Various Temperatures

Test Temperature	Y.S. in MPa for Various Solution Treatments (30 Minutes Followed by an Air Cool)*			
	1395 K (2050°F)	1420 K (2100°F)	1450 K (2150°F)	1475 K (2200°F)
Room	855 (124) 835 (121) 815 (118) 805 (117) 805 (117)	780 (113)	770 (112)	715 (104) 710 (103) 710 (103)
920 K (1200°F)	780 (113) 760 (110)			595 (86) 570 (83)
1035 K (1400°F)	780 (113) 765 (111)			640 (93) 620 (90)
1145 K (1600°F)	635 (92) 635 (92) 565 (82) 550 (80)	625 (91) 580 (84) 565 (82) 530 (77) 510 (74)	580 (84) 550 (80)	595 (86) 595 (86) 570 (83) 560 (81)
1255 K (1800°F)	325 (47) 290 (42) 255 (37)	250 (36)	255 (37)	260 (38)

Numbers in parentheses are KSI.
* All samples aged at 1170 K (1650°F) for 4 hours.

Table 10

Effect of Solution Treatment Temperature Upon Tensile Elongation

Test Temperature	Tensile Elongation in Percent for Various Solution Treatments (30 Minutes Followed by an Air Cool)*			
	1395 K (2050°F)	1420 K (2100°F)	1450 K (2150°F)	1475 K (2200°F)
Room	25 24 22 21 20	16	13	11 10 8
920 K (1200°F)	17 17			14 7
1035 K (1400°F)	16 15			6 4
1145 K (1600°F)	13 12 12 11	13 10 10 8 7	11 10	9 9 8 7
1255 K (1800°F)	15 11 10	12	14	10

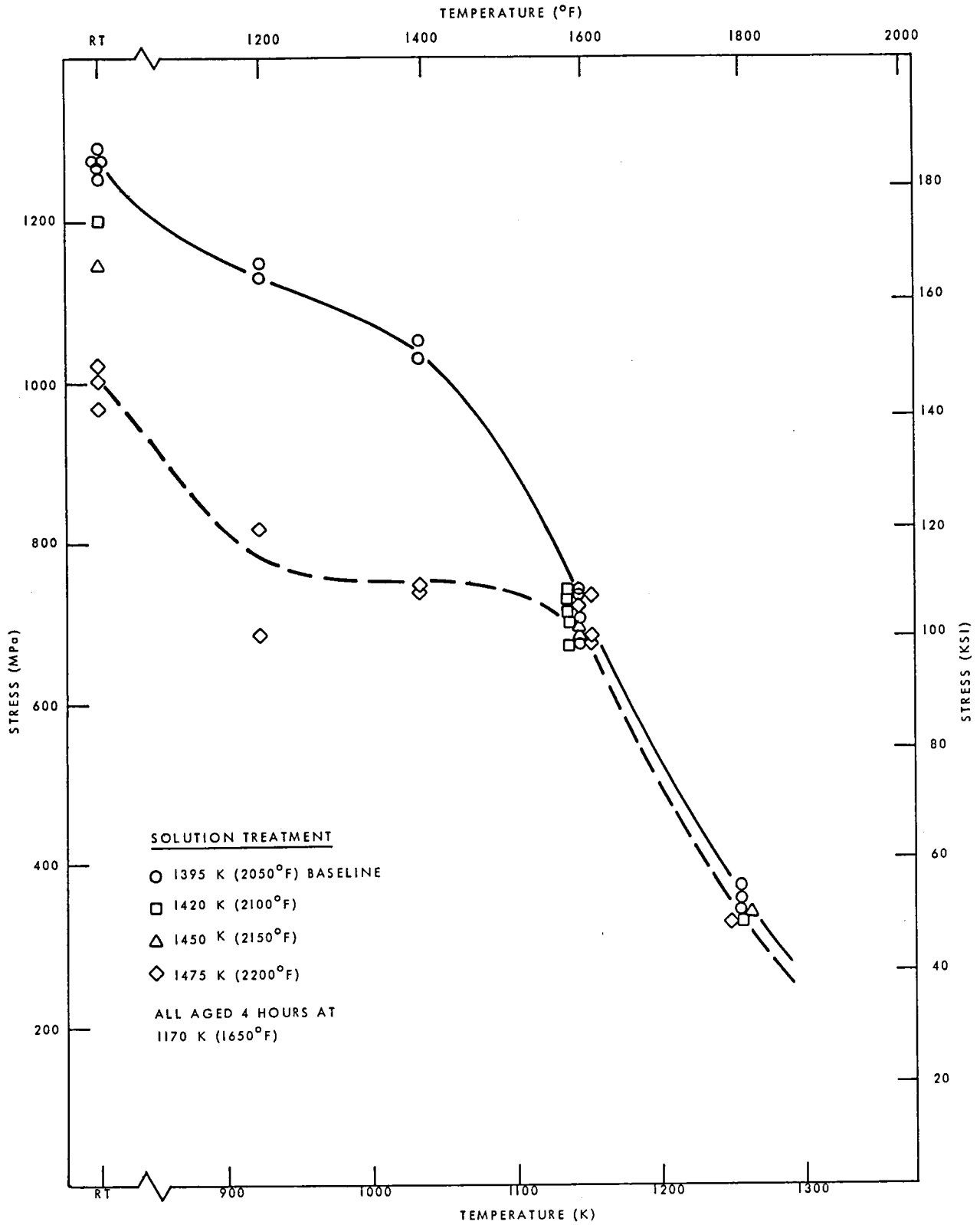* All samples aged at 1170 K (1650°F) for 4 hours.

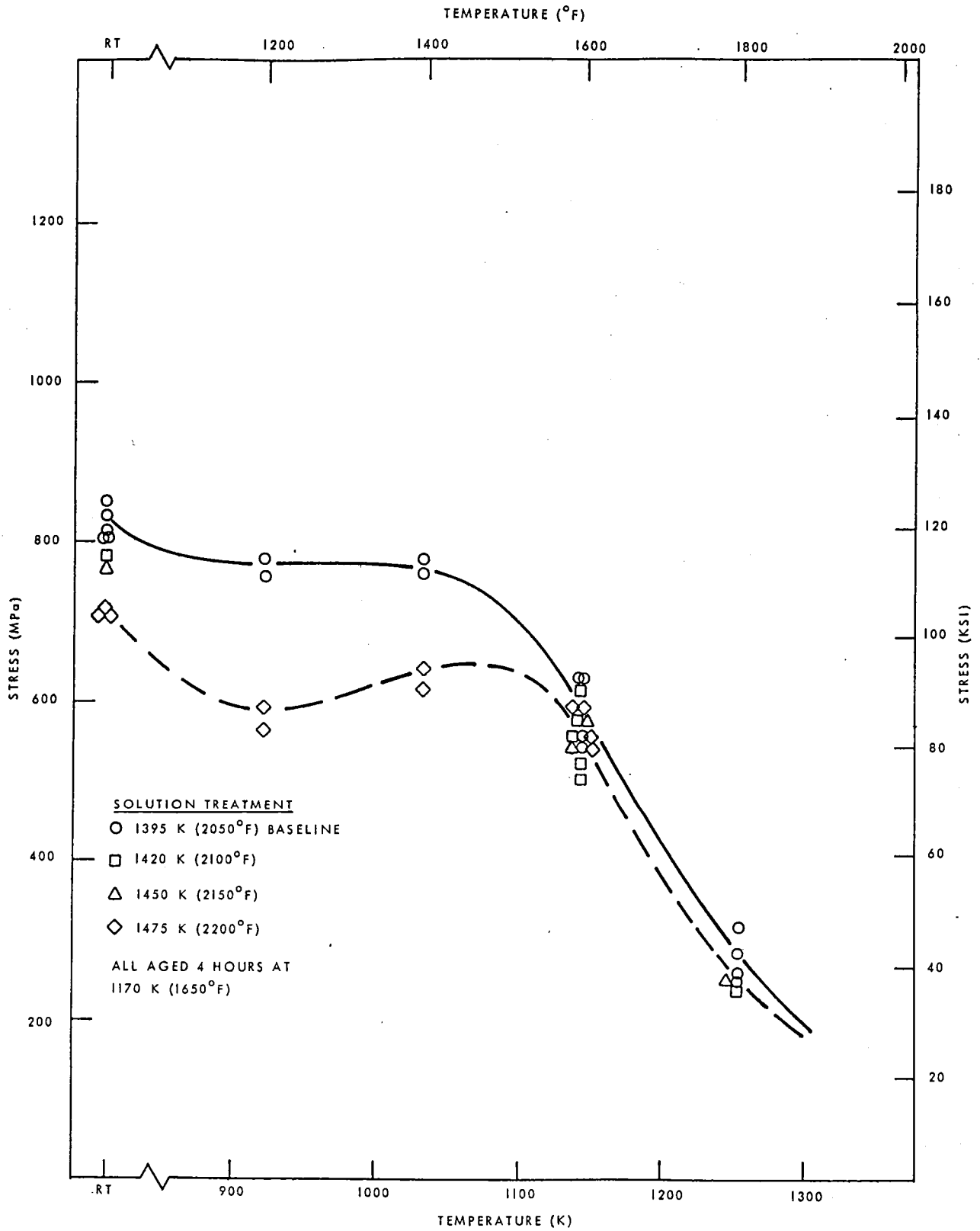FIGURE 11: EFFECT OF SOLUTION TREATMENT TEMPERATURE UPON ULTIMATE TENSILE STRENGTH.

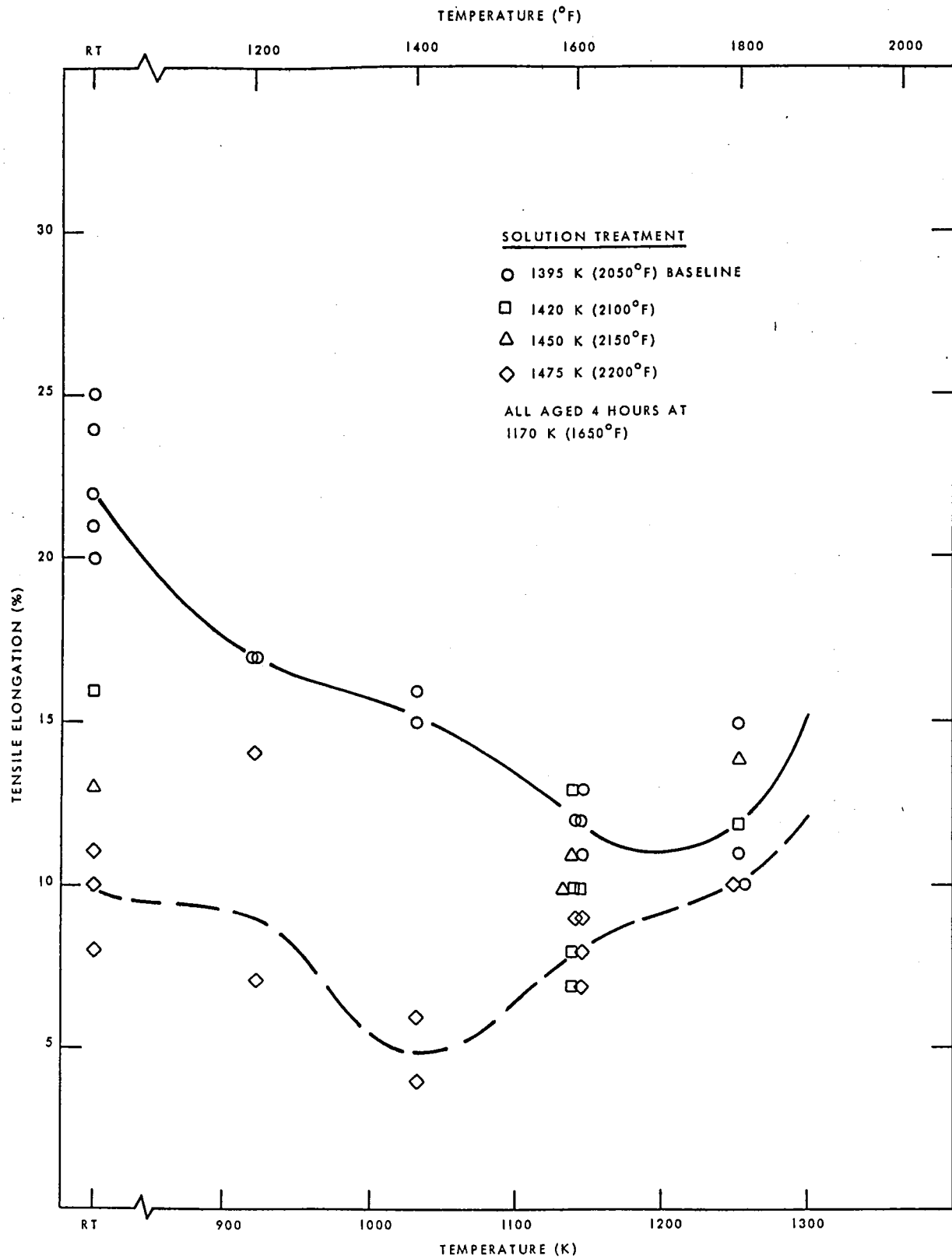FIGURE 12: EFFECT OF SOLUTION TREATMENT TEMPERATURE UPON 0.2% OFFSET YIELD STRENGTH.

FIGURE 13: EFFECT OF SOLUTION TREATMENT TEMPERATURE UPON TENSILE ELONGATION.

(2150°F) were evaluated at room temperature, 1145 K (1600°F), and 1255 K (1800°F). As shown in Table 11, these results indicate no beneficial effects at the temperatures tested when compared with the single solution treatment.

<div align="center">

3.3 Aging Treatment Studies for
1475 K (2200°F) Solution Treatment

</div>

Having noted the potentially large increase in creep strength to be had as a function of increasing the grain size with a 1475 K (2200°F) solution treatment, studies were undertaken to examine the influence of single-step and two-step aging treatments upon the 1145 K (1600°F) tensile properties. The objective was to develop a treatment with improved tensile ductility over that achieved with the standard age of 1170 K (1650°F)/4 hours/AC, hereafter referred to as "Heat Treatment A." Once again, at the time these studies were initiated, the shift in the tensile ductility minimum from 1145 K (1600°F) to 1035 K (1400°F) brought on by solution treating at 1475 K (2200°F) was not known to have occurred.

Initial Studies:

Following solution treatment at 1475 K (2200°F), single-step aging treatments at temperatures ranging from 1035 K (1400°F) to 1255 K (1800°F) were applied to material for 24 hours for temperatures less than 1170 K (1650°F) and eight hours for temperatures greater than 1170 K (1650°F). These materials were then subjected to two or more transverse tensile tests at 1145 K (1600°F) using the specimen configuration shown in Appendix A. Results of these tests are given in Table 12. From the results, it is clear that, compared to the standard Heat Treatment A only the 24-hour age at 1145 K (1600°F) produced a higher tensile elongation at 1145 K (1600°F), and that was only a very slight improvement. (Hereafter, the 24-hour age at 1145 K (1600°F) is referred to as "Heat Treatment B.") All of the other treatments resulted in lower 1145 K (1600°F) tensile ductilities.

In an effort to promote increased tensile ductility by selectively coarsening the size of the gamma prime precipitates and, thus, weakening the matrix to some extent, double-step aging treatments involving a higher temperature, first-step age were evaluated. It was hoped that such a treatment might be developed which would increase intermediate temperature tensile ductility without sacrificing creep strength. Samples were given a first-step age of eight hours at temperatures ranging from 1200 K (1700°F) to 1255 K (1800°F) and then air cooled. A second 24-hour aging treatment was then applied at 1090 K (1500°F) or, in some cases, 1035 K (1400°F) or 1145 K (1600°F).

Two or more transverse tensile tests at 1145 K (1600°F) were performed for each heat treatment using the specimen configuration described in Appendix A. Results of these tests are presented in Table 13. As can be seen, a slight improvement in 1145 K (1600°F) tensile ductility was achieved with the 1225 K (1750°F)/8 hour/AC plus 1090 K (1500°F)/24 hour/AC treatment, hereafter referred to as "Heat Treatment C" and the

Table 11

Effect of Inserting a Furnace Cool to a Second Solution Treatment
Temperature Upon the Tensile Properties of Material Solution Treated
at 1475 K (2200°F) and 1450 K (2150°F)

Heat Treatment	Test Temperature	U.T.S. (MPa)	(KSI)	0.2% Y.S. (MPa)	(KSI)	El. (%)
1475 K (2200°F)/30 Minutes/FC to 1310 K (1900°F)/4 Hours/AC + 1170 K (1650°F)/4 Hours/AC	Room	885	128	685	99	6
	1145°K (1600°F)	715	104	595	86	7
		695	101	605	88	7
	1255°K (1800°F)	345	50	260	38	10
1450 K (2150°F)/30 Minutes/FC to 1310 K (1900°F)/4 Hours/AC + 1170 K (1650°F)/4 Hours/AC	Room	1095	159	740	107	13
	1145°K (1600°F)	690	100	565	82	9
		710	103	625	91	10
	1255 K (1800°F)	345	50	260	38	10

Table 12

Effect of Single Step Aging Treatment Temperature Upon the 1145 K (1600°F) Tensile Properties of Material Solution Treated at 1475 K (2200°F) for 30 Minutes

Aging Temperature	Time (Hours)	UTS (MPa)	(KSI)	0.2% Y.S. (MPa)	(KSI)	Elongation (%)
1035 K (1400°F)	24	725	105	615	89	4
		725	105	620	90	4
1090 K (1500°F)	24	750	109	615	89	7
		740	107	585	85	5
		730	106	580	84	6
1145 K (1600°F)	24	705	102	515	75	9
		740	107	540	78	10
1170 K (1650°F)	4	745	108	595	86	9
		730	106	595	86	9
		695	101	570	83	7
		685	99	560	81	8
1225 K (1750°F)	8	710	103	540	78	5
		650	94	495	72	7
1240 K (1775°F)	8	585	85	460	67	5
		635	92	505	73	5
		710	103	530	77	5
		710	103	545	79	7
1255 K (1800°F)	8	670	97	540	78	4
		685	99	540	78	6
		585	85	515	75	4
		615	89	530	77	3

Table 13

Effect of Various Two Step Aging Treatments Upon the 1145 K (1600°F) Tensile Properties of Material Solution Treated at 1475 K (2200°F) for 30 Minutes

Aging Treatment	UTS (MPa)	(KSI)	0.2% Y.S. (MPa)	(KSI)	Elongation (%)
1200 K (1700°F)/8 Hours/AC +	655	95	440	64	7
1090 K (1500°F)/24 Hours/AC	670	97	450	65	9
1225 K (1750°F)/8 Hours/AC +	685	99	475	69	7
1090 K (1500°F)/24 Hours/AC	635	92	425	62	10
	655	95	405	59	9
	670	97	420	61	11
1240 K (1775°F)/8 Hours/AC +	685	99	460	67	10
1090 K (1500°F)/24 Hours/AC	675	98	470	68	9
	655	95	435	63	12
	675	98	470	68	10
1255 K (1800°F)/8 Hours/AC +	660	96	460	67	9
1090 K (1500°F)/24 Hours/AC	635	92	455	66	4
1240 K (1775°F)/8 Hours/AC +	650	94	415	60	6
1145 K (1600°F)/24 Hours/AC	640	93	405	59	5
1255 K (1800°F)/8 Hours/AC +	615	89	385	56	3
1145 K (1600°F)/24 Hours/AC	650	94	395	57	4
1240 K (1775°F)/8 Hours/AC +	705	102	510	74	6
1035 K (1400°F)/24 Hours/AC	675	98	550	80	2

1240 K (1775°F)/8 hour/AC plus 1090 K (1500°F)/24 hour/AC treatment, hereafter referred to as "Heat Treatment D." All the other treatments produced 1145 K (1600°F) tensile ductilities inferior to the 1170 K (1650°F) Heat Treatment A.

In order to assess the effects of these two aging treatments and that of the single-step 1145 K (1600°F) Heat Treatment B upon creep properties, duplicate transverse creep tests were performed at 1255 (1800°F) at a stress of 28 MPa (14 KSI) using the specimen configuration shown in Appendix A. Results of these tests are given in Table 14, along with the earlier results for Heat Treatment A for comparison. An advantage is evident for the two-step Heat Treatment C over the other treatments.

Characterization of First-Selected Heat Treatment:

As a consequence of its creep strength advantage at 1255 K (1800°F) and its equivalence to Heat Treatments B and D in 1145 K (1600°F) tensile ductility, Heat Treatment C was selected for in-depth property characterization. Transverse creep and stress rupture testing using the specimen configuration shown in Appendix A was initiated at a variety of temperature and stress combinations. At the same time, transverse tensile testing using the same specimen configuration was initiated for temperatures ranging from room temperature to 1365 K (2000°F).

Results of the creep tests are presented in Table 15 and those for stress rupture in Table 16. The values for 0.5 percent and 1.0 percent creep strength are shown plotted as a function of the Larson-Miller parameter in Figures 14 and 15, respectively. Rupture strength is plotted similarly in Figure 16.

From an examination of Figures 14 and 15, it can be concluded that Heat Treatment C produces a significant increase in creep strength over the baseline material for Larson-Miller parameters greater than about P_K = 24,000 (P_R = 43,000), but reduces creep strength at Larson-Miller parameters below that level. This behavior is understandable, in that the beneficial effect of increased grain size should only be manifested above the equicohesive temperature where creep occurs by the mechanism of grain boundary sliding. Below the equicohesive temperature, intragranular dislocation slip is the predominant form of creep deformation. In this regime, coarser grain sizes and weakened matrix effects of the heat treatment should lower creep strength, as is observed. It is somewhat surprising to note from Figure 16 that the stress rupture properties achieved for Heat Treatment C are no better than the baseline material. This is only of passing interest, however, as the limiting design criteria of importance for avoiding component failure in the present study is low strain creep.

Though only limited creep data were generated for Heat Treatment C (the reason for this will become clear presently), a statistical evaluation was performed. The results of this evaluation are given in Table 17, and the lines shown in Figures 14 and 15 for the 0.5 percent and 1.0 percent creep strengths are, in fact, the regression lines calculated

Table 14

1255 K/28 MPa (1800°F/4 KSI) Creep Properties for Selected Heat Treatments

Heat Treatment		Hours to % Creep	
		0.5%	1.0%
1475 K (2200°F)/30 Minutes/AC		140	252
+ 1170 K (1650°F)/4 Hours/AC (A)		140	266
	log Av.*	140	259
1475 K (2200°F)/30 Minutes/AC		142	240
+ 1145 K (1600°F)/24 Hours/AC (B)		156	289
	log Av.	149	263
1475 K (2200°F)/30 Minutes/AC		169	283
+ 1225 K (1750°F)/8 Hours/AC (C)		194	329
+ 1090 K (1500°F)/24 Hours/AC			
	log Av.	181	305
1475 K (2200°F)/30 Minutes/AC		137	234
+ 1240 K (1775°F)/8 Hours/AC (D)		169	303
+ 1090 K (1500°F)/24 Hours/AC			
	log Av.	152	266

* Antilog of the average of the logarithms of the test hours.

Table 15

Summary of Creep Test Data for 1475 K (2200°F)/30 Minutes/AC + 1225 K (1750°F)/8 Hours/AC + 1090 K (1500°F)/24 Hours/AC Heat Treatment

Test Temperature	Test Stress (MPa)	Test Stress (KSI)	Hours to % Creep 0.5%	Hours to % Creep 1.0%
1035 K (1400°F)	380	55	3	9
1090 K (1500°F)	315	46	2	6
	260	38	16	38
	205	30	104	180
1145 K (1600°F)	170	25	26	44
	145	21	51	94
	115	17	94	222
1200 K (1700°F)	97	14	33	57
	76	11	97	174
	55	8	283	540

Table 16

Summary of Stress Rupture Test Data for
1475 K (2200°F)/30 Minutes/AC + 1225 K (1750°F)/8 Hours/AC
+ 1090 K (1500°F)/24 Hours/AC Heat Treatment

Test Temperature	Test Stress (MPa)	(KSI)	Life (Hours)	El. (%)
1035 K (1400°F)	550	80	3	13
	550	80	2	14
	515	75	8	17
	450	65	39	12
1145 K (1600°F)	205	30	41	13
	205	30	40	11
1255 K (1800°F)	83	12	9	6
	83	12	6	6

P = T(°R)(20 + Log t)

BASELINE MATERIAL

HEAT TREATMENT C

HEAT TREATMENT C
= 1475 K (2200°F)/30 MINUTES/AC
+ 1225 K (1750°F)/8 HOURS/AC
+ 1090 K (1500°F)/24 HOURS/AC

STRESS (MPa)

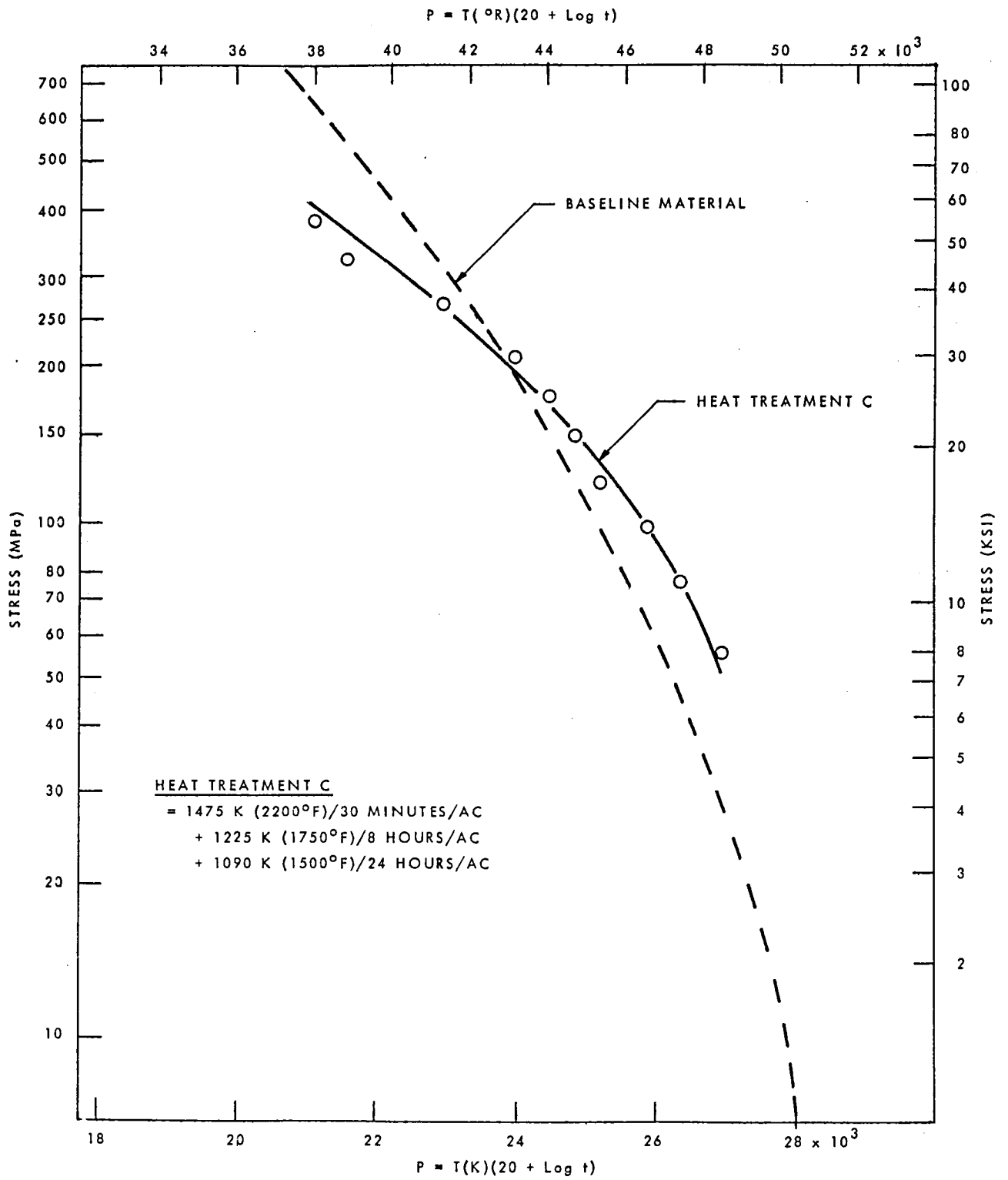STRESS (KSI)

P = T(K)(20 + Log t)

FIGURE 14: 0.5% CREEP STRENGTH OF MATERIAL GIVEN HEAT TREATMENT C AS A FUNCTION
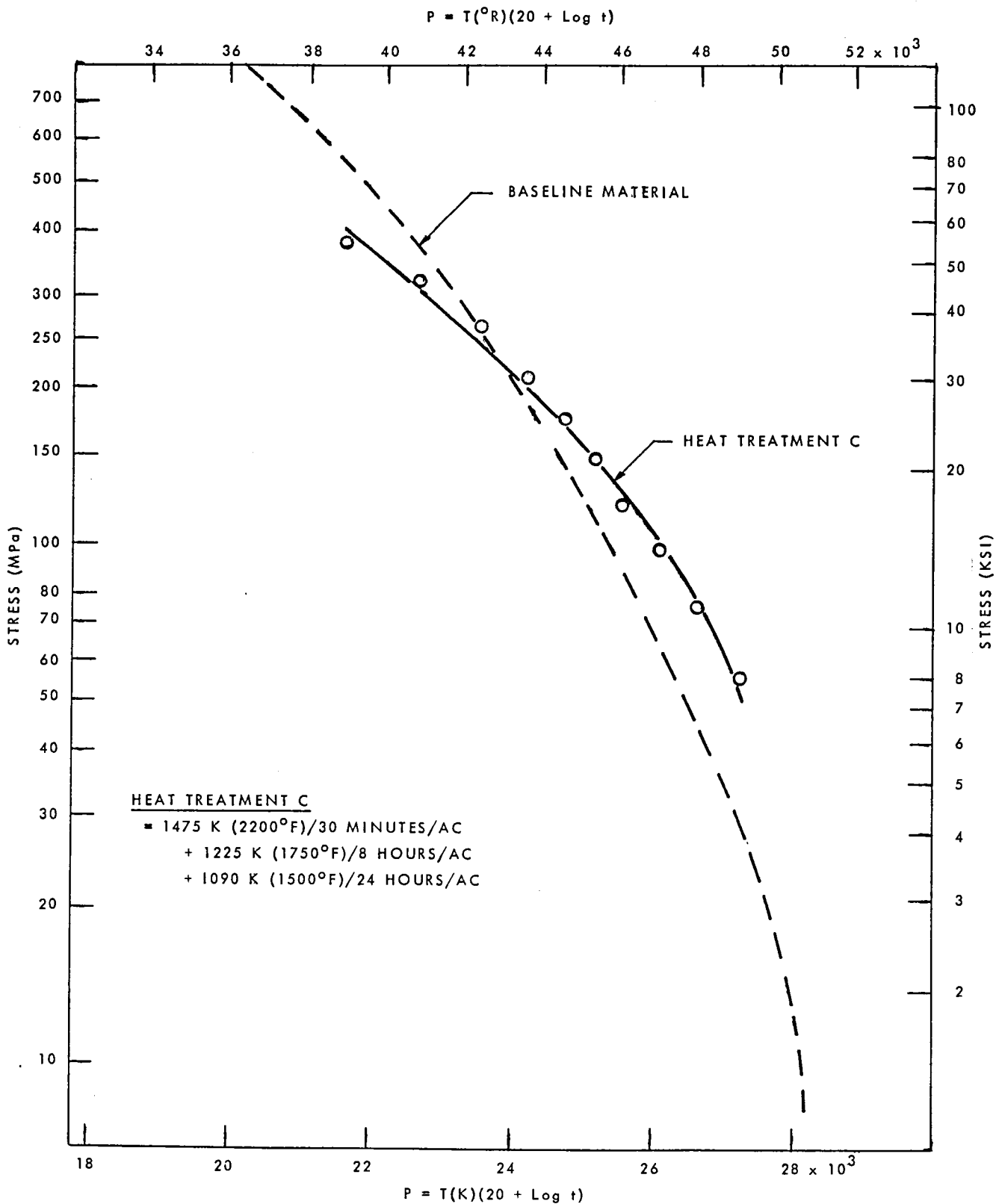OF LARSON-MILLER PARAMETER.

FIGURE 15: 1.0% CREEP STRENGTH OF MATERIAL GIVEN HEAT TREATMENT C AS A FUNCTION OF LARSON-MILLER PARAMETER.
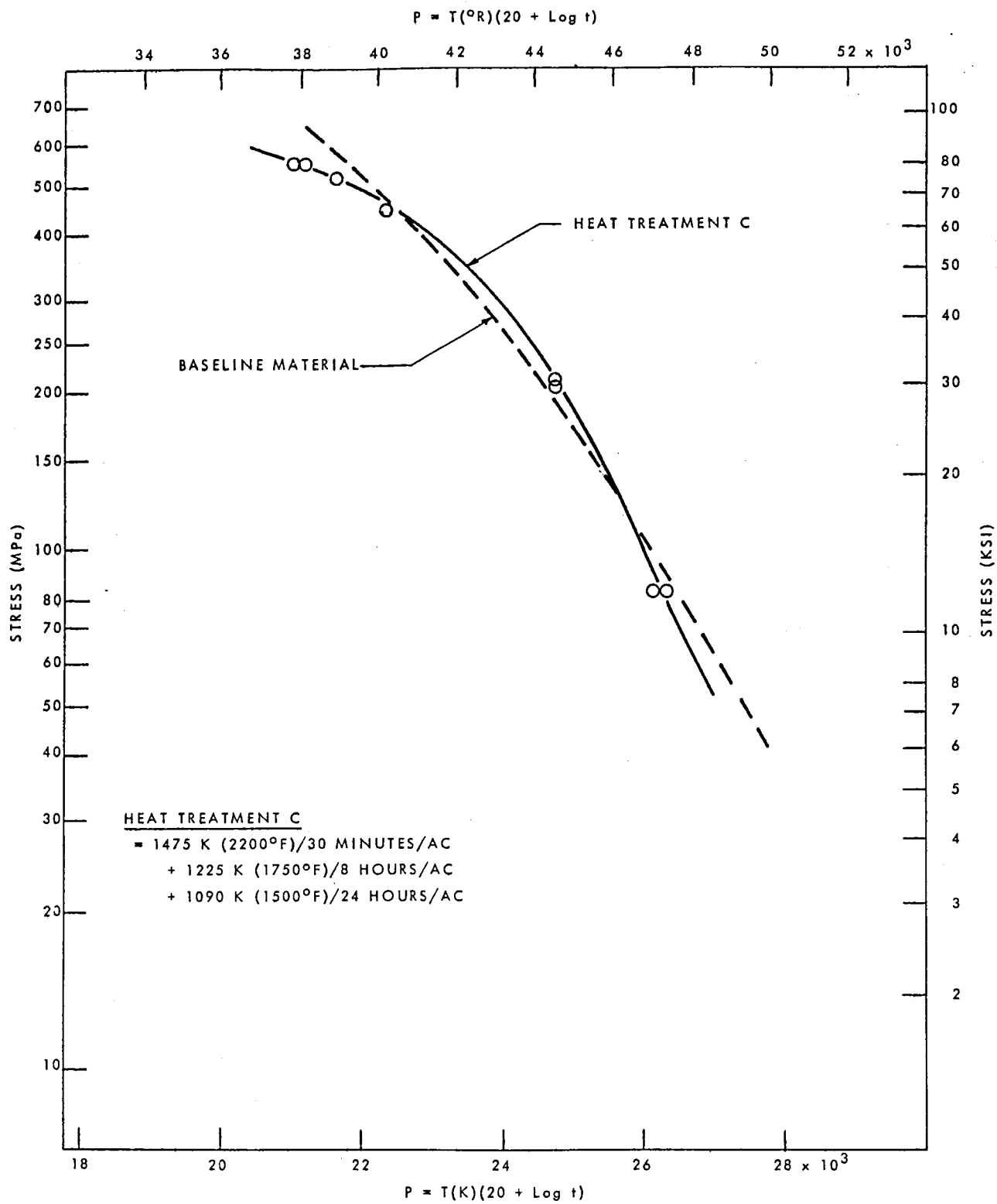
FIGURE 16: STRESS RUPTURE STRENGTH OF MATERIAL GIVEN HEAT TREATMENT C AS A FUNCTION OF LARSON-MILLER PARAMETER.

Table 17

Larson-Miller Parameter Analysis for Creep Data Obtained from
Material Given a 1475 K (2200°F)/30 Minutes/AC + 1225 K (1750°F)/
8 Hours/AC + 1090 K (1500°F)/24 Hours/AC Heat Treatment

Regression Equation: $P = T (20.0 + \log t) = C_1 + C_2 \log S + C_3 (\log S)^2$

A. Where T = Temperature (K)
        S = Stress (MPa)
        t = Time to given creep strain (hours)

Percent Creep	Equation Constants			Std. Error of Estimate (LM Parameter Units)	Multiple Correlation Coefficient	Index of Determination
	C_1	C_2	C_3			
0.5	17,333.0	13,557.9	−4,654.5	189.1	.996	.990
1.0	20,619.6	10,616.4	−3,931.6	147.5	.997	.993

B. Where T = Temperature (°R)
        S = Stress (KSI)
        t = Time to given creep strain (hours)

Percent Creep	Equation Constants			Std. Error of Estimate (LM Parameter Units)	Multiple Correlation Coefficient	Index of Determination
	C_1	C_2	C_3			
0.5	45,772.0	10,354.0	−8,378.0	340.4	.996	.990
1.0	48,163.1	7,241.3	−7,076.9	265.6	.997	.993

in the analysis. Largely as a consequence of the limited number of data points (ten), the fit of the regression lines to the observed data is quite good.

Although many additional creep tests for material given Heat Treatment C had been planned, such testing was abandoned once the results of the elevated temperature tensile tests performed upon material so heat treated were obtained. The results for transverse tensile tests performed using the specimen configuration shown in Appendix A are presented in Table 18. The low values for tensile elongation at room temperature, 920 K (1200°F), and 1035 K (1400°F) are striking.

Tensile ductility, ultimate tensile strength, and 0.2 percent offset yield strength as a function of temperature for material given Heat Treatment C are plotted in comparison to the baseline material and material given Heat Treatment A in Figures 17, 18, and 19, respectively. From the curves in Figure 17, it is clear that, instead of improving the tensile ductility minimum, Heat Treatment C yielded material with a ductility worse than that produced for Heat Treatment A. From examining Figure 19, it can also be discerned that Heat Treatment C lowered the yield strength at 1145 K (1600°F) without gaining much in the way of ductility.

Similar behaviors were found for Heat Treatments B and D. Tensile properties for the former are given in Table 19. A comparison of the room-temperature tensile ductilities achieved with Heat Treatments A, B, C, and D is shown in Figure 20. It is clearly shown that the effort aimed at improving the heat treatment to this point in the study had resulted in reducing the tensile ductility!

Re-examination of Furnace Cool Approach:

In light of the tensile results obtained for Heat Treatments B, C, and D, it was decided to re-evaluate the possible beneficial effects to be had by employing a furnace cool following a solution treatment at 1475 K (2200°F). Instead of furnace cooling to a second solution treatment temperature above the gamma prime solvus, however, it was decided to furnace cool directly to the aging temperature range.

Results of duplicate transverse and room-temperature tensile tests (performed using a specimen configuration as shown in Appendix A) for material given a variety of aging treatments following a furnace cool from 1475 K (2200°F) are presented in Table 20. From these data, it is clear that the furnace cool approach produces reasonably consistent results almost independent of aging treatment. For the treatment involving furnace cooling to 1225 K (1750°F)/4 hours/AC + 1090 K (1500°F)/24 hours/AC, hereafter known as Heat Treatment E, the tensile ductility at room temperature, as shown in Figure 20, is better than those achieved using Heat Treatments C or D. It is also at least as good as that for Heat Treatment B, though still a bit lower than that for Heat Treatment A.

48

Table 18

Tensile Properties for Material Solution Treated at 1475 K (2200°F)/30 Minutes/Air Cool and Aged at 1225 K (1750°F)/8 Hours/Air Cool Plus 1090 K (1500°F)/24 Hours/Air Cool

| Test Temperature	UTS (MPa)	UTS (KSI)	0.2% Y.S. (MPa)	0.2% Y.S. (KSI)	Elongation (%)
Room	870	126	725	105	4
	890	129	730	106	4
	870	126	685	99	2
	905	131	655	95	3
920 K (1200°F)	855	124	660	96	5
	950	138	710	103	5
	850	123	620	90	4
	915	133	625	91	5
1035 K (1400°F)	805	117	660	96	2
	855	124	640	93	4
	840	122	620	90	9
	855	124	615	89	2
1145 K (1600°F)	685	99	475	69	7
	635	92	425	62	10
	655	95	405	59	9
	670	97	420	61	11
1255 K (1800°F)	305	44	220	32	12
	415	60	260	38	12
	365	53	275	40	6
	470	68	325	47	10
1365 K (2000°F)	145	21	90	13	16
	110	16	55	8	23
	105	15	55	8	23
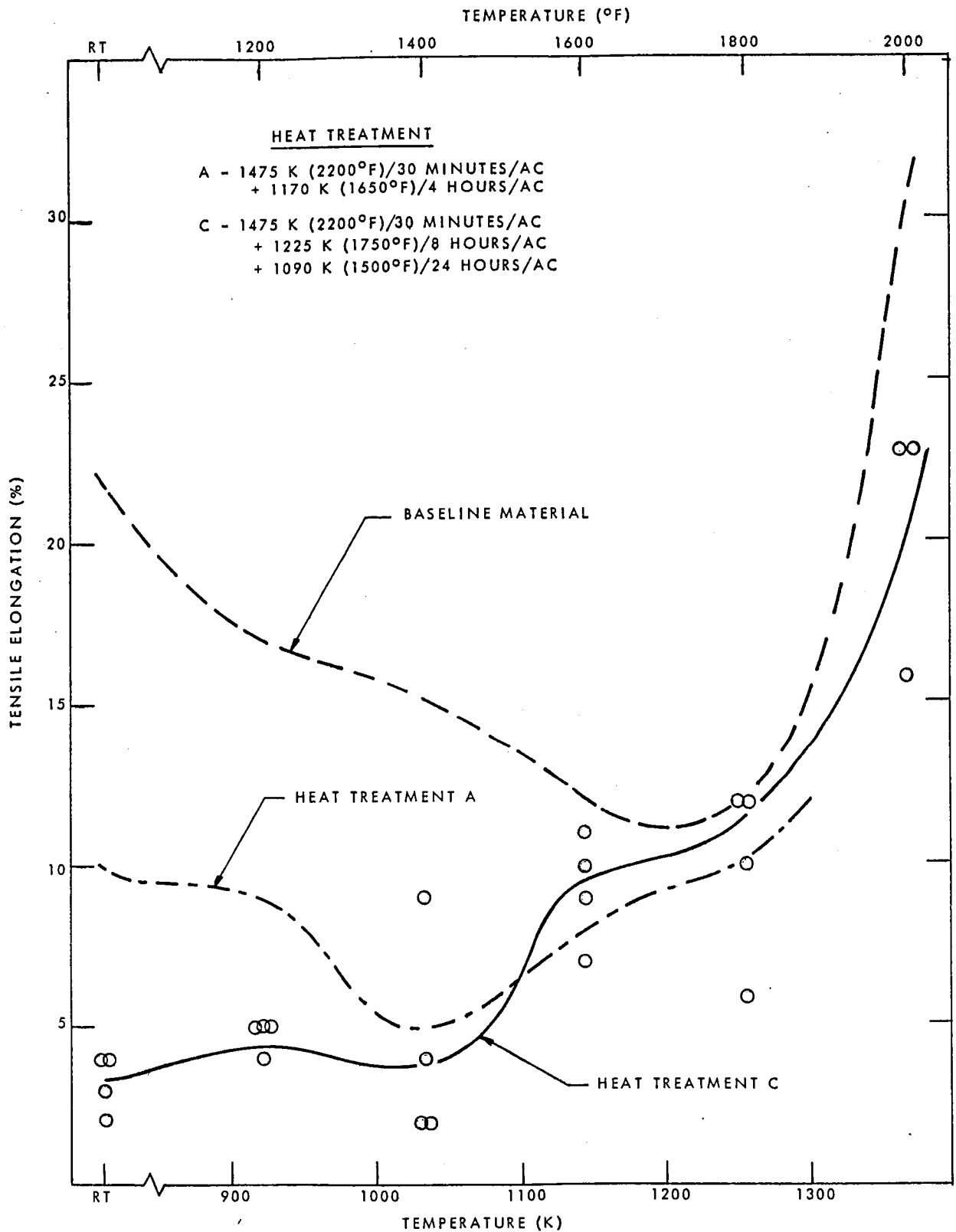
FIGURE 17: COMPARISON OF AGING TREATMENT EFFECTS UPON TENSILE DUCTILITY.
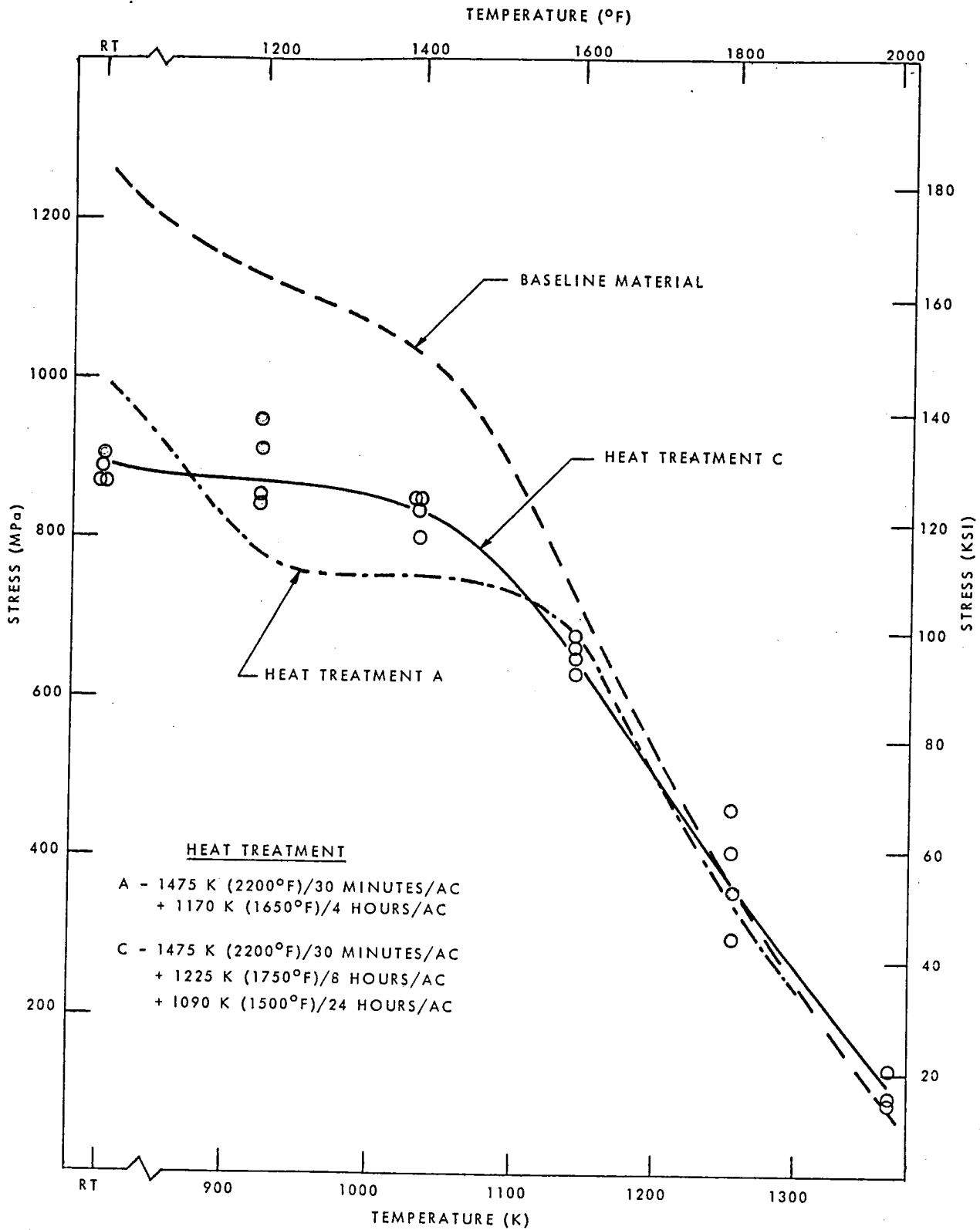
FIGURE 18: COMPARISON OF AGING TREATMENT EFFECTS UPON ULTIMATE TENSILE STRENGTH.

51

TEMPERATURE (°F)

HEAT TREATMENT

A – 1475 K (2200°F)/30 MINUTES/AC
  + 1170 K (1650°F)4 HOURS/AC

C – 1475 K (2200°F)/30 MINUTES/AC
  + 1225 K (1750°F)/8 HOURS/AC
  + 1090 K (1500°F)/24 HOURS/AC

BASELINE MATERIAL

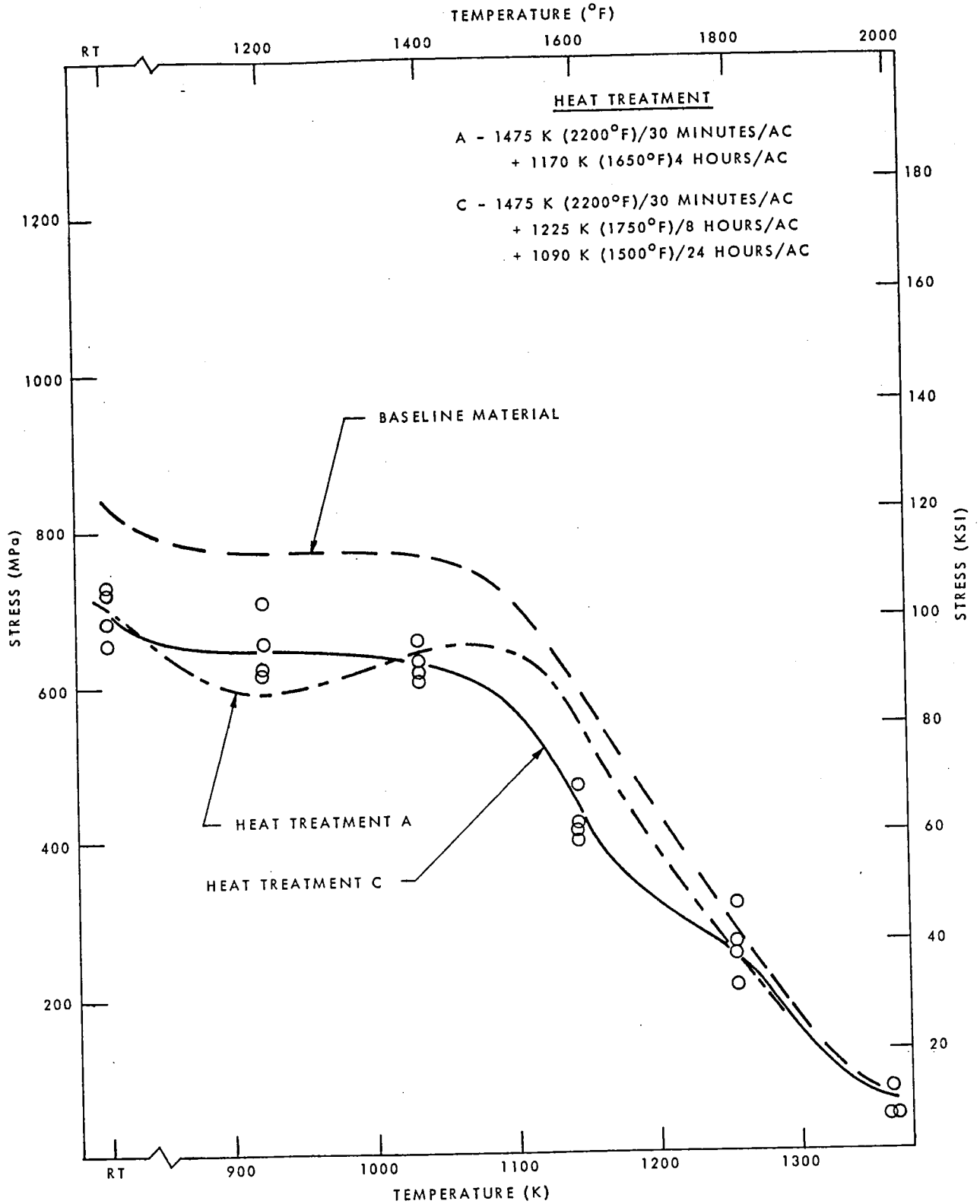HEAT TREATMENT A

HEAT TREATMENT C

TEMPERATURE (K)

FIGURE 19: COMPARISON OF AGING TREATMENT EFFECTS UPON 0.2% OFFSET
YIELD STRENGTH.

Table 19

Tensile Properties for Material Solution Treated
at 1475 K (2200°F)/30 Minutes/Air Cool and Aged
at 1145 K (1600°F)/24 Hours/Air Cool

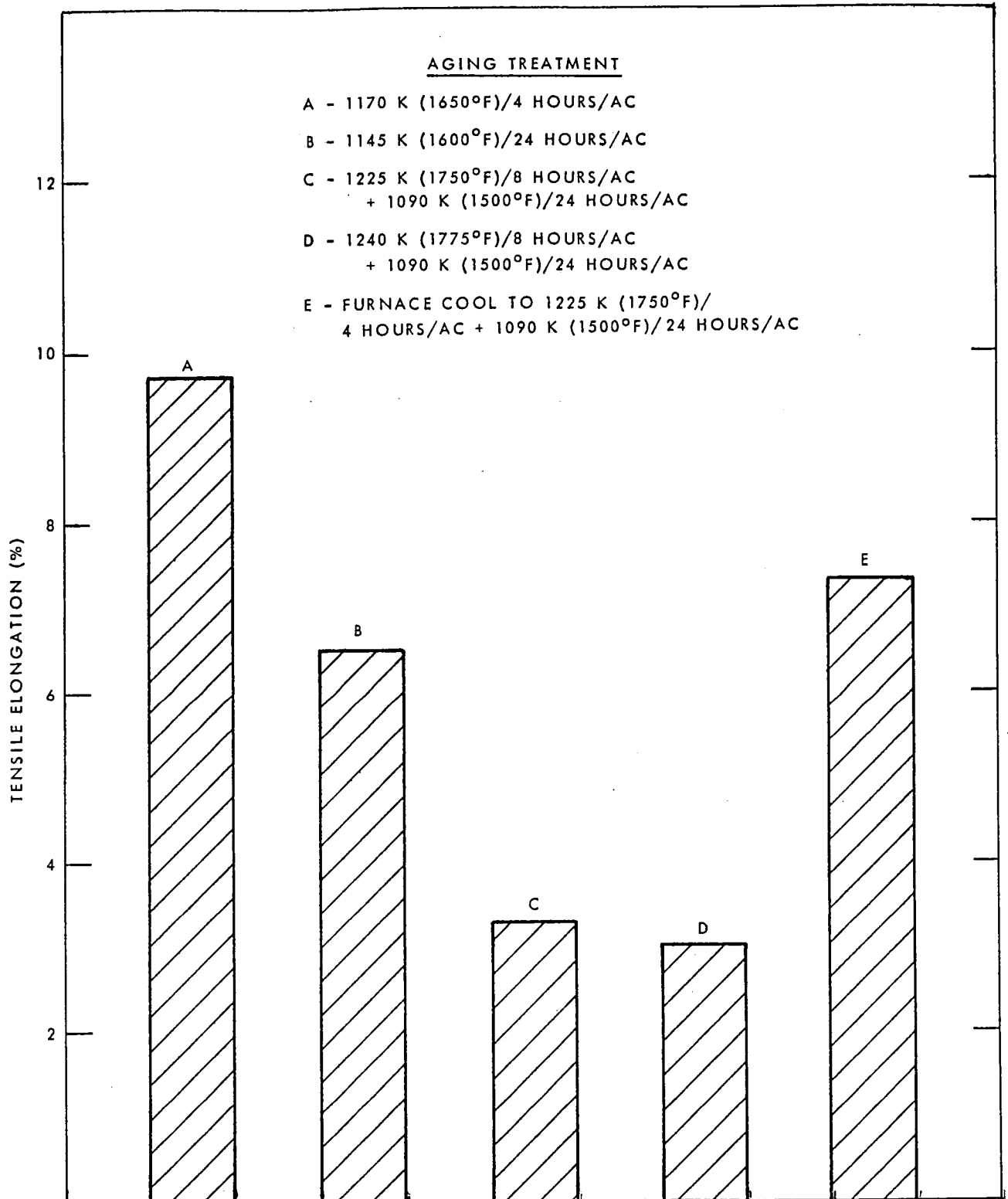| Test Temperature	UTS (MPa)	(KSI)	0.2% Y.S. (MPa)	(KSI)	Elongation (%)
Room	890	129	695	101	7
	875	127	695	101	6
920 K (1200°F)	795	115	635	92	7
	770	112	620	90	7
1035 K (1400°F)	825	120	670	97	5
	815	118	660	96	4
1145 K (1600°F)	705	102	515	75	9
	740	107	540	78	10

FIGURE 20: ROOM TEMPERATURE TENSILE ELONGATION FOR VARIOUS AGING
TREATMENTS FOLLOWING SOLUTION TREATMENT AT 1475 K (2200°F).

Table 20

Room-Temperature Tensile Properties of Materials Given
Various Aging Treatments Including a Furnace Cool Following
Solution Treatment at 1475 K (2200°F) for 30 Minutes

Aging Treatment	UTS		0.2% Y.S.		Elongation
	(MPa)	(KSI)	(MPa)	(KSI)	(%)
FC to 1225 K (1750°F)/4 Hrs./AC	850	123	635	92	8
+ 1090 K (1500°F)/24 Hrs./AC	905	131	650	94	7
	915	133	655	95	7
FC to 1225 K (1750°F)/8 Hrs./FC	915	133	635	92	8
to 1090 K (1500°F)/24 Hrs./AC	835	121	640	93	5
FC to 1225 K (1750°F)/1 Hr./FC	910	132	635	92	7
to 1090 K (1500°F)/24 Hrs./AC	855	124	635	92	6
FC to 1225 K (1750°F)/1 Hr./AC	965	140	675	98	8
+ 1090 K (1500°F)/24 Hrs./AC	940	136	675	98	7
FC to 1090 K (1500°F)/24 Hrs./AC	885	128	670	97	7
	960	139	675	98	8

Characterization of Second-Selected Heat Treatment:

Based upon the results obtained for the room-temperature tensile properties of material given Heat Treatment E, two or more transverse tensile tests were performed at each of a variety of temperatures ranging from 920 K (1200°F) to 1365 K (2000°F). Once again, the specimen geometry shown in Appendix A was used. Results for these tests are presented in Table 21. Plots of tensile ductility, ultimate tensile strength, and 0.2 percent offset yield strength versus temperature are shown in Figures 21, 22, and 23, respectively.

It is apparent from the data in Table 21 that Heat Treatment E results in a substantial increase in tensile ductility relative to the previously considered heat treatments. This is clearly illustrated in Figure 21, where a comparison is made to both Heat Treatment A and the baseline material. At temperatures of 1035 K (1400°F) or above, Heat Treatment E results in a tensile elongation equivalent to or better than that for the baseline material and far higher than that for Heat Treatment A. At temperatures below 1035 K (1400°F), however, the ductility produced with Heat Treatment E is significantly lower than that for the baseline material, but still reasonably equivalent to that for Heat Treatment A.

An examination of Figures 22 and 23 reveals that, as the price for the improvement obtained in the tensile ductility at temperatures at or above 1035 K (1400°F), the ultimate tensile strength and 0.2 percent offset yield strength are significantly lower than those obtained with Heat Treatment A. This is unfortunate; but, since the limiting design criteria for the application in question is, once again, low strain creep, the loss of tensile strength properties should not be important.

In an effort to better understand what had been achieved by the adoption of the furnace cool approach embodied in Heat Treatment E, replica electron microscopy was performed for material subjected to both Heat Treatment E and Heat Treatment D (air cool and reheat approach). Also, x-ray analysis of extracted residues was performed for both heat treatments using the same procedures as described in Section 3.2.

Typical electron photomicrographs for material subjected to Heat Treatments D and E are shown in Figures 24 and 25, respectively. The condition of the grain boundary carbide in the microstructure produced with the air cool and reheat approach of Heat Treatment D is not much different than that observed for Heat Treatment A, which was shown in Figure 7d. The carbides are not discrete particles, but are a continuous grain boundary film. The size of the gamma prime particles is only slightly coarser.

Contrasting with this is the structure of the material given Heat Treatment E, as shown in Figure 25. Here, the grain boundaries are considerably thicker relative to the structure shown in Figure 24, but the carbides are neither cellular nor continuous in morphology. Rather, the grain boundary structure is typified by a mixture of what appears to be two distinct types of discrete carbides and interspersed gamma prime.

Table 21

Tensile Properties for Material Solution Treated
at 1475 K (2200°F)/30 Minutes/Furnace Cool to 1225 K (1750°F)
and Aged at 1225 K (1750°F)/4 Hours/Air Cool Plus
1090 K (1500°F)/24 Hours/Air Cool

Test Temperature	UTS		0.2% Y.S.		Elongation
	(MPa)	(KSI)	(MPa)	(KSI)	(%)
Room	850	123	635	92	8
	905	131	650	94	7
	915	133	655	95	7
920 K (1200°F)	930	135	620	90	7
	945	137	580	84	11
1035 K (1400°F)	820	119	625	91	16
	785	114	580	84	14
1145 K (1600°F)	485	70	395	57	16
	495	72	380	55	15
	485	70	360	52	12
	490	71	380	55	14
	490	71	350	51	16
	485	70	345	50	19
1255 K (1800°F)	230	33	170	25	22
	220	32	160	23	17
	240	35	205	30	17
	235	34	180	26	−
1365 K (2000°F)	55	8	41	6	36
	55	8	34	5	31

TEMPERATURE (°F)

HEAT TREATMENT

A – 1475 K (2200°F)/30 MINUTES/AC
+ 1170 K (1650°F)/4 HOURS/AC

E – 1475 K (2200°F)/30 MINUTES/FC
TO 1225 K (1750°F)/4 HOURS/AC
+ 1090 K (1500°F)/24 HOURS/AC

BASELINE MATERIAL

HEAT
TREATMENT E

HEAT TREATMENT A

TENSILE ELONGATION (%)
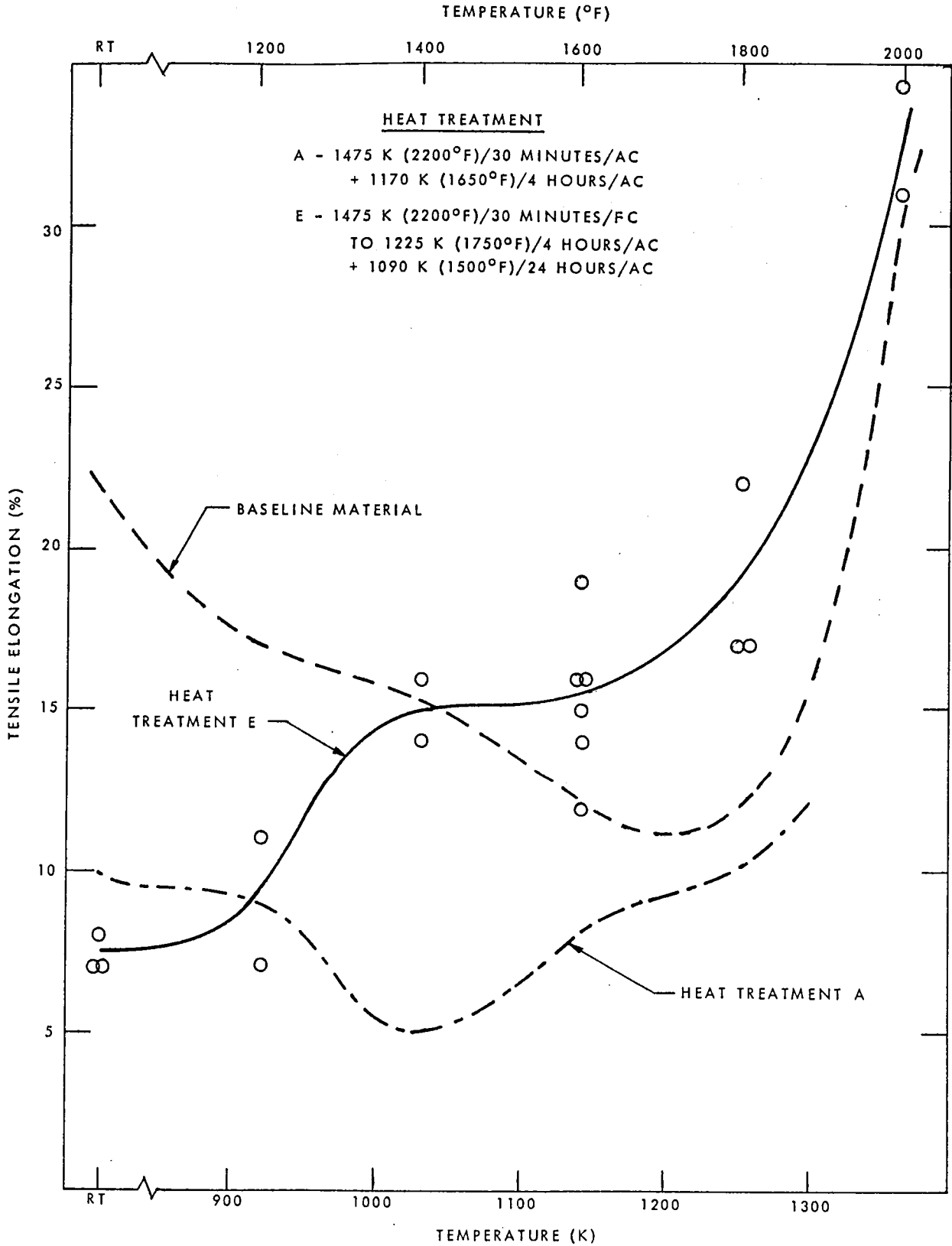
TEMPERATURE (K)

FIGURE 21: COMPARISON OF AGING TREATMENT EFFECTS UPON TENSILE DUCTILITY.

58
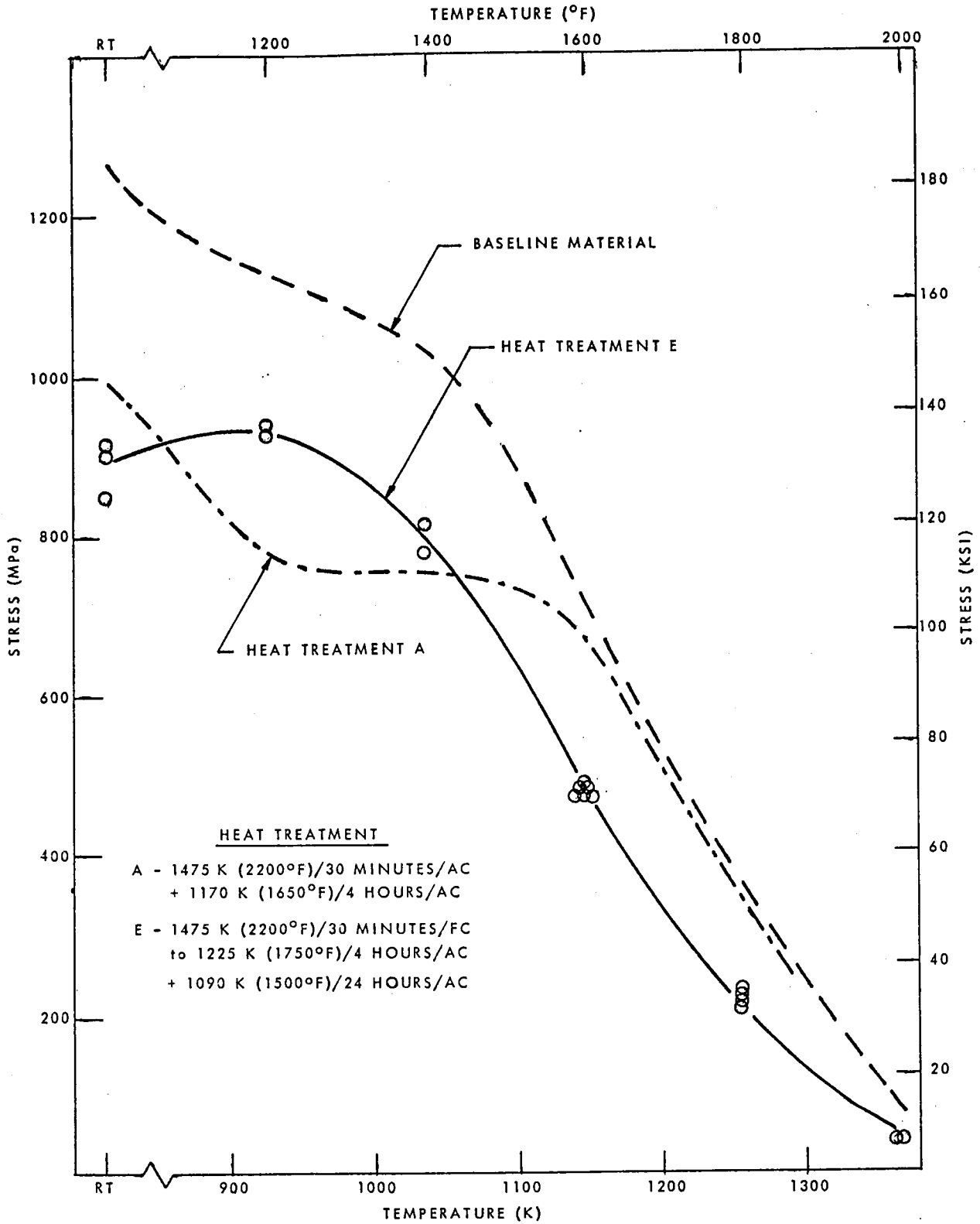
FIGURE 22: COMPARISON OF AGING TREATMENT EFFECTS UPON ULTIMATE
TENSILE STRENGTH.

59

FIGURE 23: COMPARISON OF AGING TREATMENT EFFECTS UPON 0.2% OFFSET YIELD STRENGTH.

60

Figure 24: Microstructure following 1475 K (2200°F)/30 minute/AC + 1240 K (1775°F)/8 hour/AC + 1090 K (1500°F)/24 hour/AC heat treatment. 9400X.

Figure 25: Microstructure following 1475 K (2200°F)/30 minute/FC to 1225 K (1750°F)/4 hour/AC + 1090 K (1500°F)/24 hour/AC heat treatment. 9400X.

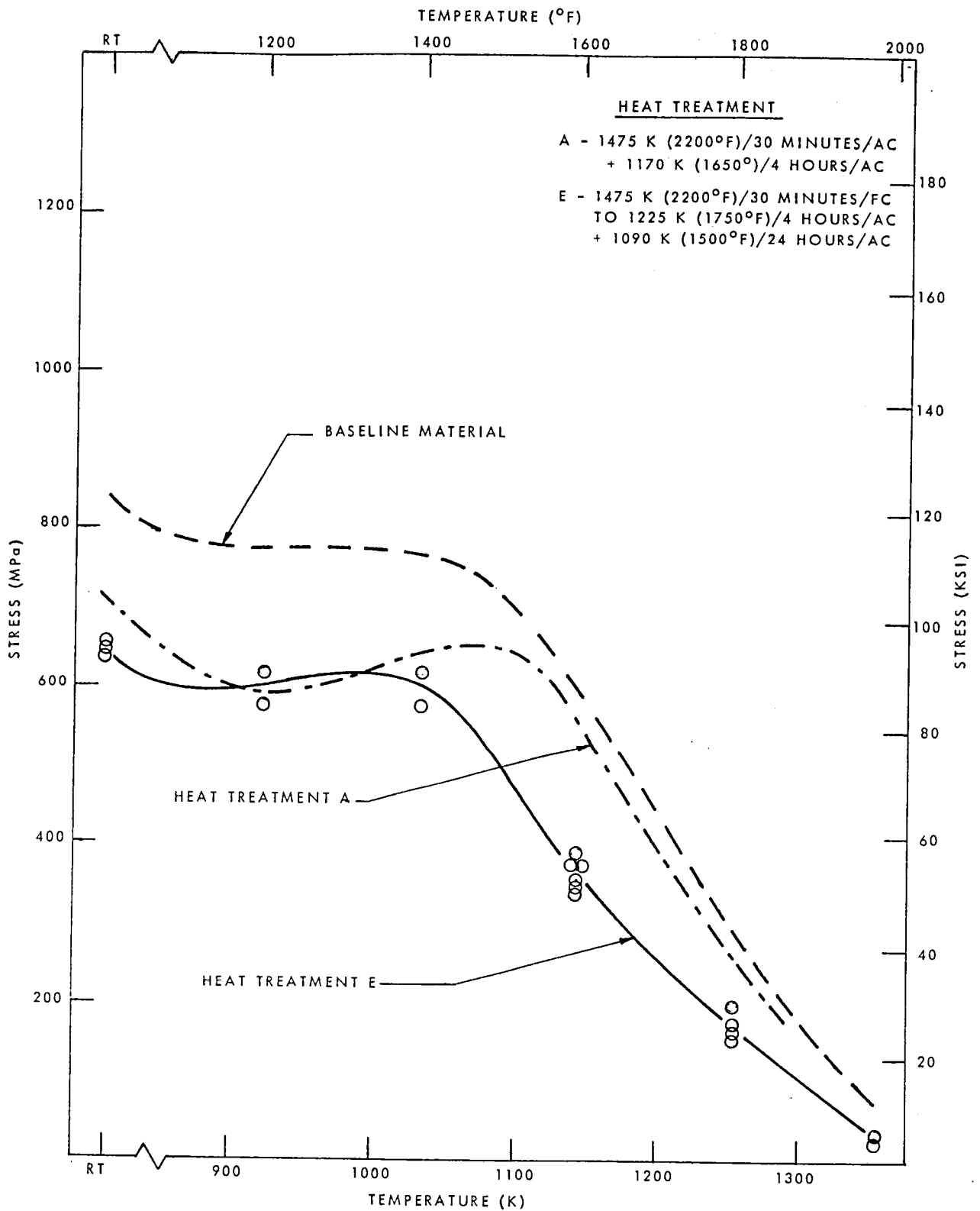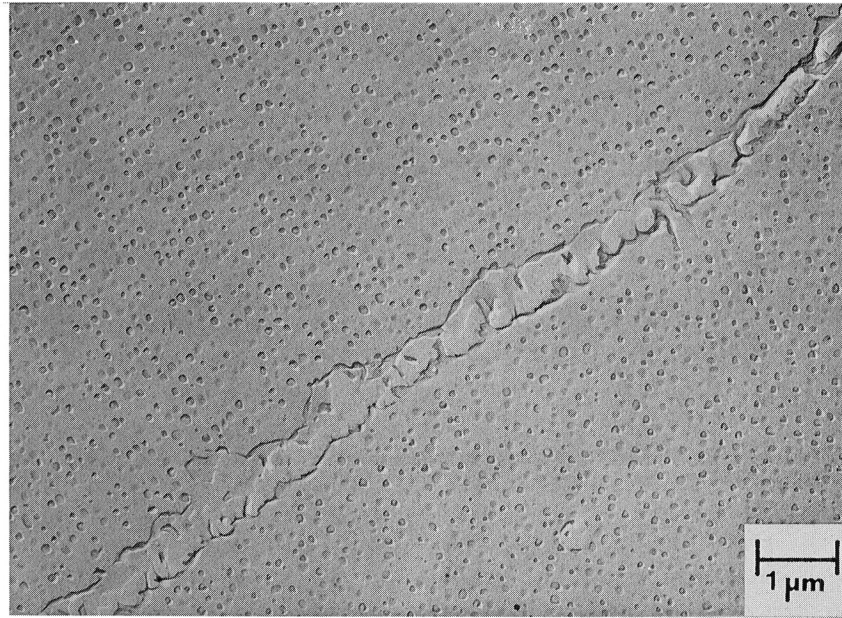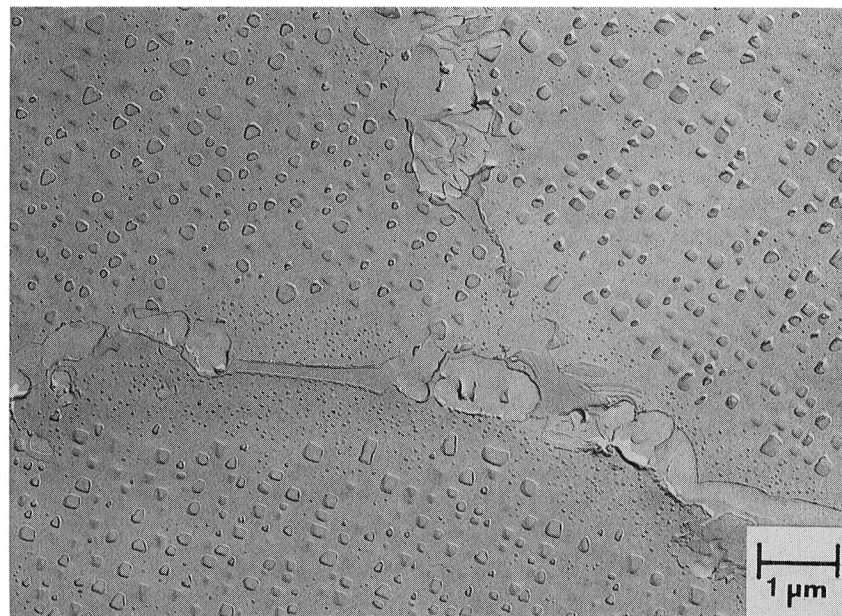There are also a few elongated particles which resemble mu phase in appearance (a nickel- and molybdenum-rich phase similar to Fe_7Mo_6 in stoichiometry and crystal structure) in the boundaries. The success of the furnace cool approach in promoting the reprecipitation of dissolved M_6C carbides as new, discrete M_6C carbide particles is also confirmed by the results of the x-ray analysis of the extracted residues shown in Table 6. Note the shift back toward strong M_6C carbide intensity and weak $M_{23}C_6$ carbide intensity for Treatment E versus Treatment D.

The morphology of the gamma prime precipitates in the matrix for the structure shown in Figure 25 is considerably different from that shown in Figure 24 or Figure 7d. Away from the grain boundaries, gamma prime particles about four or more times the size of those shown in Figure 24 are observed, while next to the grain boundaries very fine gamma prime precipitates are found. The larger particles undoubtedly precipitated during the furnace cool to 1225 K (1750°F) and grew during the first aging step at that temperature. This apparently resulted in a gamma prime precipitate-depleted zone adjacent to the boundaries in which the fine gamma prime precipitated during the subsequent second aging step at 1090 K (1500°F).

This observed structure is consistent with the fact that during the furnace cool from 1475 K (2200°F) M_6C carbides would begin to precipitate at the grain boundaries as the temperature fell below 1435 K (2125°F). These carbides are rich in molybdenum, so the adjacent matrix could be expected to be depleted in that element. Loomis et al. (ref. 20) established that molybdenum has a pronounced positive effect upon the gamma prime solvus temperature in nickel-base superalloys; so, this depletion of molybdenum content near the grain boundaries could be enough to lower the local gamma prime solvus temperature below the 1225 (1750°F) first-step aging temperature. This would account for the absence of coarse gamma prime particles near the boundaries. Of course, even in these depleted zones, fine gamma prime precipitates would be expected to precipitate at the 1090 K (1500°F) second-step aging temperature.

The structure generated by Heat Treatment E apparently allows for increased grain boundary strength relative to that of the matrix and thus accounts for the improved ductility. This is so because the weaker matrix can deform to a greater extent before work hardening to the point where the grain boundary strength is exceeded. In this respect, Heat Treatment E fulfills the aims established for the two-step aging treatment approach for 1475 K (2200°F) solution-treated material, though, admittedly, room-temperature tensile ductility is marginal.

In view of this, broad spectrum transverse creep and stress rupture testing was performed for material given Heat Treatment E using the specimen configuration shown in Appendix A. Results for 0.5 percent and 1.0 percent creep tests performed at temperatures ranging from 1035 K (1400°F) to 1255 K (1800°F) are presented in Table 22. Values for 0.5 percent creep strength as a function of the Larson-Miller parameter are shown plotted in Figure 26. Those for the 1.0 percent creep strength are plotted in Figure 27. Once again, creep properties are clearly enhanced

62

Table 22

Summary of Creep Test Data for 1475 K (2200°F)/
30 Minutes/FC to 1225 K (1750°F)/4 Hours/AC + 1090 K (1500°F)/
24 Hours/AC Heat Treatment

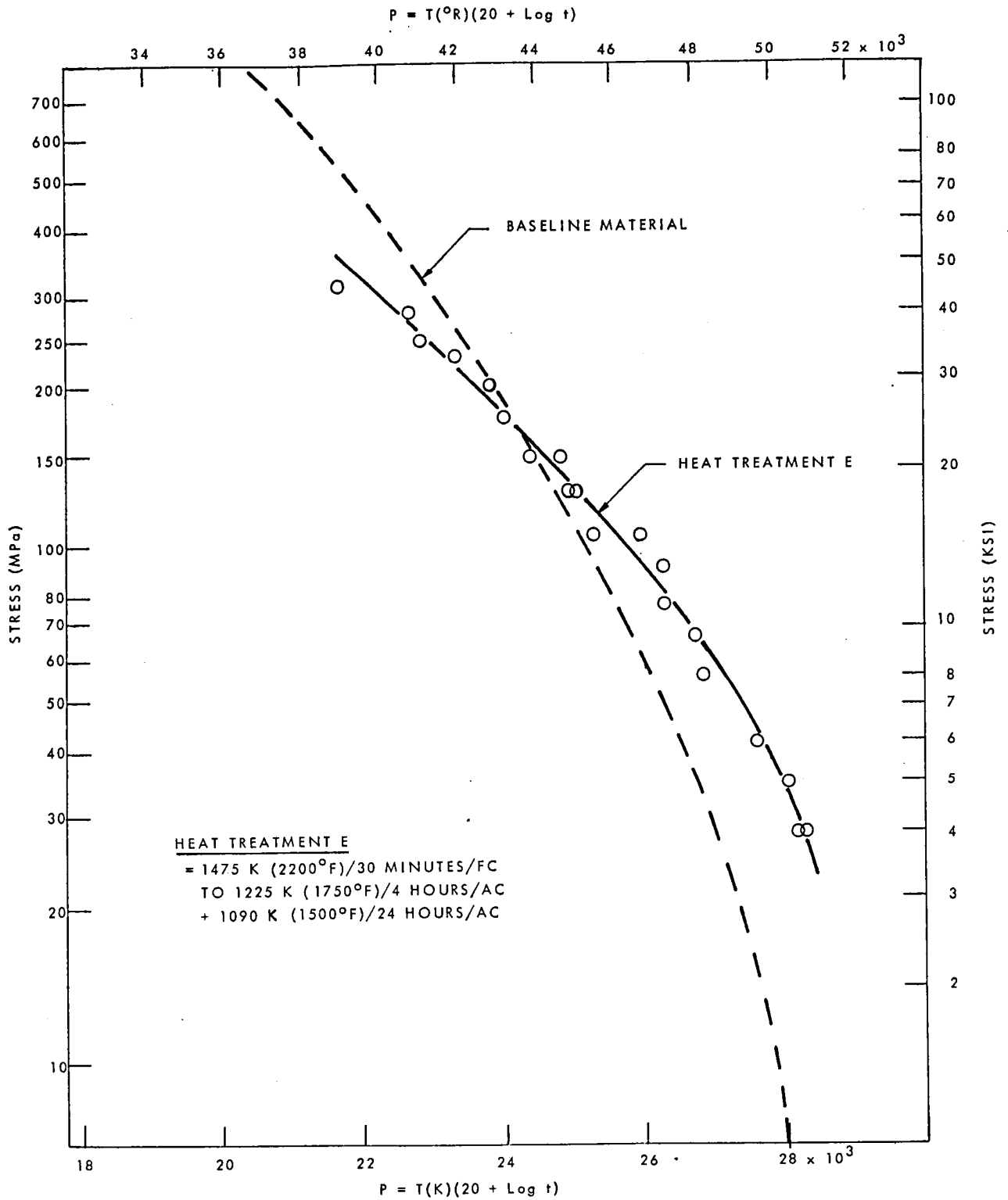| Test Temperature	Test Stress		Hours to % Creep	
	(MPa)	(KSI)	0.5%	1.0%
1035 K (1400°F)	310	45	9	28
	275	40	90	165
	240	35	118	216
1090 K (1500°F)	230	33	26	52
	200	29	68	142
	170	25	125	247
1145 K (1600°F)	145	21	52	88
	145	21	20	39
	125	18	64	124
	125	18	76	175
	105	15	117	338
1200 K (1700°F)	105	15	43	77
	90	13	77	157
	76	11	77	164
	66	9.5	190	452
	55	8	235	650
1255 K (1800°F)	41	6	94	152
	34	5	229	386
	28	4	265	403
	28	4	333	536

FIGURE 26: 0.5% CREEP STRENGTH OF MATERIAL GIVEN HEAT TREATMENT E AS A FUNCTION
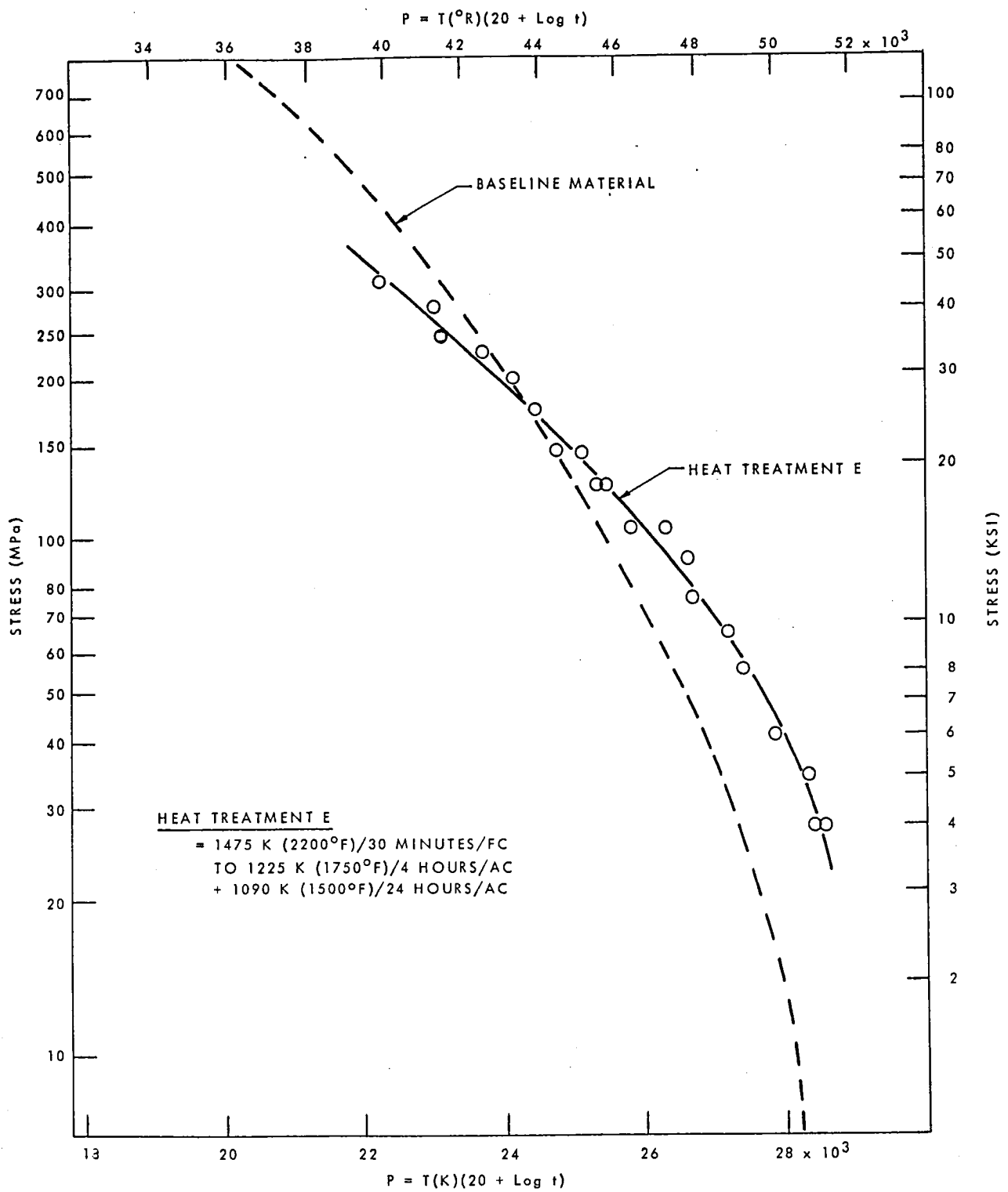OF LARSON-MILLER PARAMETER.

FIGURE 27: 1.0% CREEP STRENGTH OF MATERIAL GIVEN HEAT TREATMENT E AS A FUNCTION OF LARSON-MILLER PARAMETER.

relative to the baseline material for Larson-Miller parameters of about $P_K \geq 24,000$ ($P_R \geq 43,000$) and reduced at lower parameter levels.

Stress rupture test results are given in Table 23, and rupture strength values are plotted as a function of the Larson-Miller parameter in Figure 28. Unlike the results achieved with Heat Treatment C, Heat Treatment E does appear to produce a small increase in stress rupture strength relative to the baseline material at the higher parameter levels. Also, in comparing the stress rupture elongation results for material given Heat Treatment E to those reported for the baseline material in Table 4, some additional benefits of the new treatment may also be observed.

A statistical analysis of the creep data produced for material given Heat Treatment E was performed. The results of the regression analysis are presented in Table 24 for both the 0.5 percent and 1.0 percent creep properties. Once again, the calculated regression equations were found to provide for a very good fit to the data. The indices of determination and multiple correlation coefficients were very near to 1.0, and the Standard Error of the Estimate values were both less than 1.0 percent of the mean Larson-Miller parameter values.

A comparison of the calculated simultaneous 95 percent confidence limits for the 0.5 percent creep strength of the baseline material and material given Heat Treatment E as a function of the Larson-Miller parameter is shown in Figure 29. A similar comparison for the 1.0 percent creep strength values is shown in Figure 30. Clearly, the statistics indicate a significant improvement in the creep strength with Heat Treatment E above parameter levels corresponding to temperatures in the vicinity of 1090 K (1500°F).

3.4 Aging Treatment Studies for 1420 K (2100°F) Solution Treatment

In addition to the larger body of work performed for the 1475 K (2200°F) solution treatment, some work was done to examine the possibility of improving the creep strength of material given the less ambitious 1420 K (2100°F) solution treatment by optimizing the aging treatment(s). Samples were solution treated at 1420 K (2100°F) and then subjected to a matrix evaluation of two-step aging treatments in two phases.

In the first phase, the second aging treatment step was held constant, consisting of 1145 K (1600°F)/24 hours/AC, while the first step was varied. The first steps evaluated included eight-hour treatments at 1200 K (1700°F), 1225 K (1750°F), 1240 K (1775°F), 1255 K (1800°F), and 1270 K (1825°F), all with a subsequent air cool. Two or more transverse creep tests were conducted at 1255 K (1800°F)/21 MPa (3 KSI) using the specimen configuration shown in Appendix A.

Results of these tests are presented in Table 25. Included for reference are the results obtained for a 1145 K (1600°F)/24 hours/AC single-step aging treatment. It is clear from these results that the

66

Table 23

Summary of Stress Rupture Test Data for 1475 K (2200°F)/
30 Minutes/FC to 1225 K (1750°F)/4 Hours/AC + 1090 K
(1500°F)/24 Hour/AC Heat Treatment

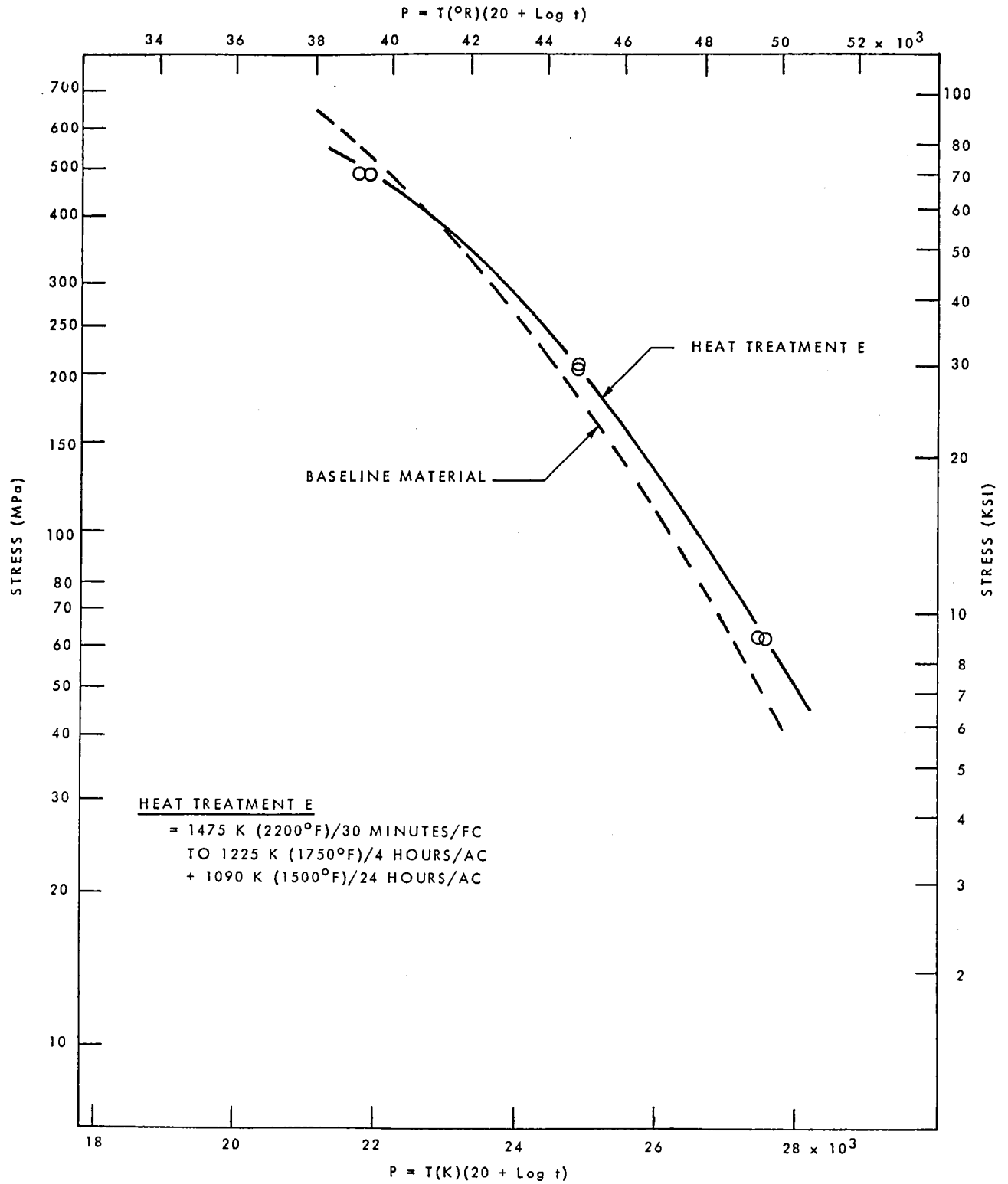| Test Temperature	Test Stress (MPa)	(KSI)	Life (Hours)	El. %
1035 K (1400°F)	485	70	11	10
	485	70	15	13
1145 K (1600°F)	205	30	55	10
	205	30	55	7
1255 K (1800°F)	62	9	88	9
	62	9	81	7

FIGURE 28: STRESS RUPTURE STRENGTH OF MATERIAL GIVEN HEAT TREATMENT E AS A
FUNCTION OF LARSON-MILLER PARAMETER.

Table 24

Larson-Miller Parameter Analysis for Creep Data Obtained from
Material Given a 1475 K (2200°F)/30 Minutes/FC to 1225 K (1750°F)/
4 Hours/AC + 1090 K (1500°F)/24 Hours/AC Heat Treatment

Regression Equation: $P = T (20.0 + \log t) = C_1 + C_2 \log S + C_3 (\log S)^2$

A. Where T = Temperature (K)
   S = Stress (MPa)
   t = Time to given creep strain (hours)

Percent Creep	Equation Constants			Std. Error of Estimate (LM Parameter Units)	Multiple Correlation Coefficient	Index of Determination
	C_1	C_2	C_3			
0.5	26,417.4	5,406.2	-2,884.2	220.5	.994	.987
1.0	25,455.3	6,733.8	-3,211.7	180.5	.996	.991

B. Where T = Temperature (°R)
   S = Stress (KSI)
   t = Time to given creep strain (hours)

Percent Creep	Equation Constants			Std. Error of Estimate (LM Parameter Units)	Multiple Correlation Coefficient	Index of Determination
	C_1	C_2	C_3			
0.5	52,060.9	1,024.7	-5,191.5	396.9	.994	.987
1.0	51,918.3	2,425.9	-5,781.0	324.9	.996	.991

FIGURE 29: COMPARISON OF 95% CONFIDENCE LIMITS FOR 0.5% CREEP STRENGTH AS A FUNCTION OF LARSON-MILLER PARAMETER. HEAT TREATMENT E VERSUS BASELINE MATERIAL.
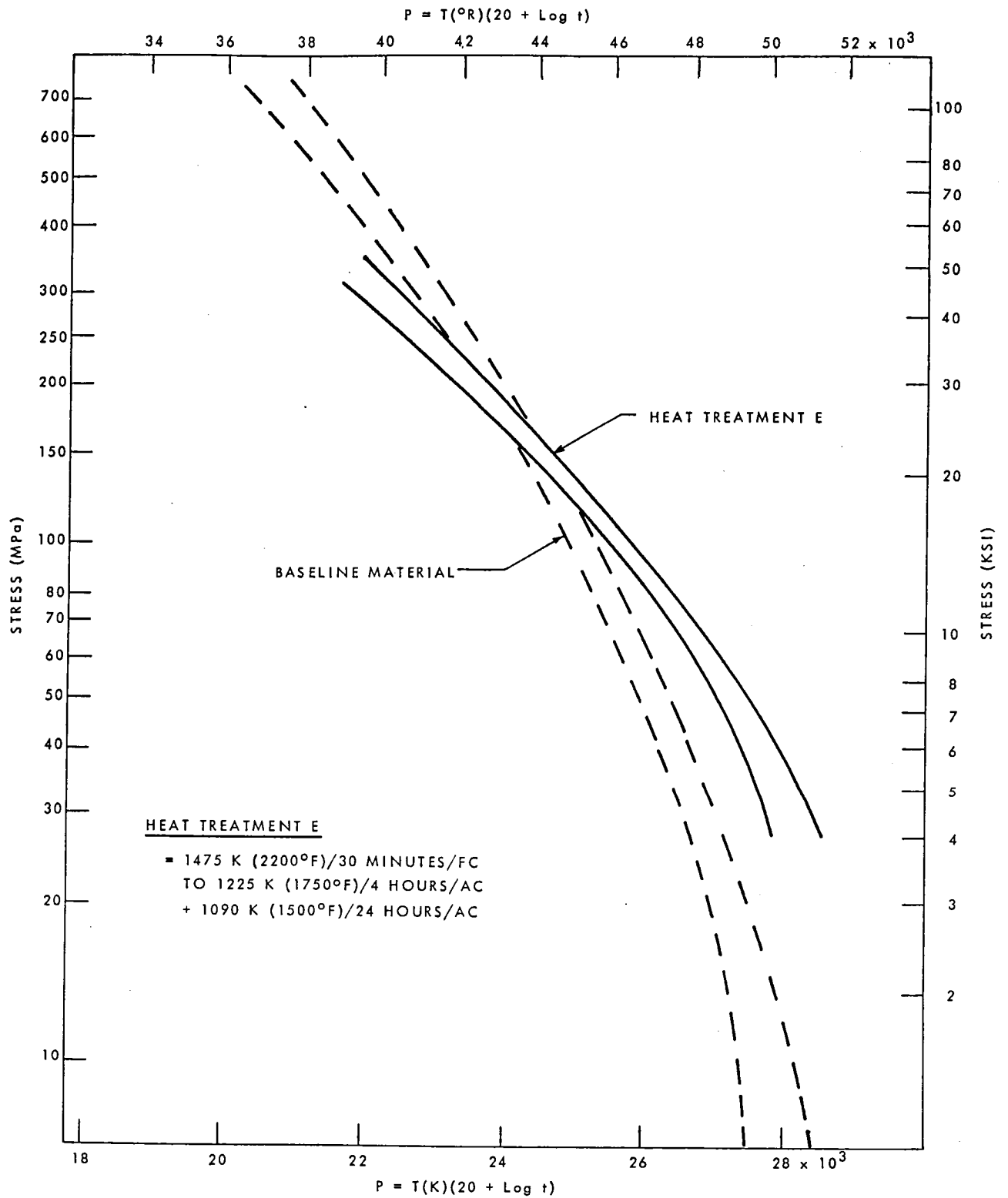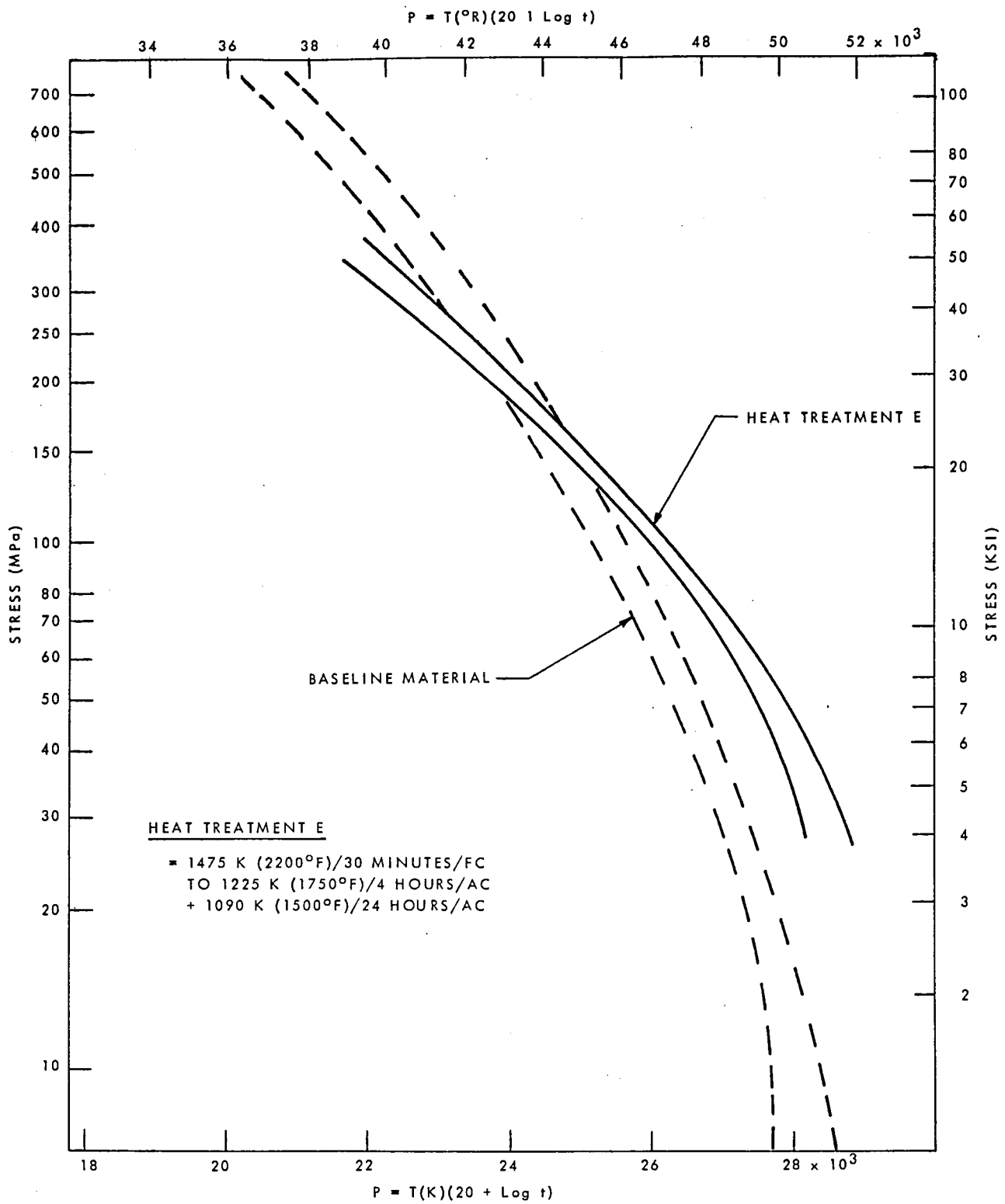
FIGURE 30: COMPARISON OF 95% CONFIDENCE LIMITS FOR 1.0% CREEP STRENGTH AS A FUNCTION OF LARSON-MILLER PARAMETER. HEAT TREATMENT E VERSUS BASELINE MATERIAL

Table 25

Effect of Intermediate Aging Treatment Upon the Creep
Properties of Material Solution Treated at 1420 K (2100°F)/
30 Minutes/AC and Final Aged at 1145 K (1600°F)/24 Hours/AC

Intermediate Aging Treatment		Hours to Percent Creep at 1255 K/21 MPa (1800°F/3 KSI)	
		0.5	1.0%
None		91	157
		73	125
	log Av.*	82	140
1200 K (1700°F)/8 Hours/AC		72	132
		68	115
	log Av.	70	123
1225 K (1750°F)/8 Hours/AC		136	238
		127	220
		138	201
		114	188
		120	206
	log Av.	127	210
1240 K (1775°F)/8 Hours/AC		212	450
		153	263
		146	242
		100	170
	log Av.	148	264
1255 K (1800°F)/8 Hours/AC		107	185
		90	160
	log Av.	98	172
1270 K (1825°F)/8 Hours/AC		129	225
		90	158
	log Av.	108	189

* Antilog of the average of the logarithms of the test hours.

highest creep strength is obtained for either a 1225 K (1750°F) or 1240 K (1775°F) first-step aging temperature.

Results for the 1145 K (1600°F) transverse tensile tests performed for material given both of these heat treatments are presented in Table 26. Both the 1225 K (1750°F) and 1240 K (1775°F) first-step treatments yielded good 1145 K (1600°F) tensile ductility, better than the values shown for material given a single-step 1170 K (1650°F)/4 hours/AC standard age. The values for the 0.2% offset yield strength are lower than those for the standard age, but again this was not considered a major concern.

Since both the average 1145 K (1600°F) yield strength and tensile ductility were a bit higher for the 1240 K (1775°F) first-step aging treatment, this temperature was selected as the constant treatment for the second phase matrix experiments. In this phase, samples solution treated at 1420 K (2100°F) and first-step aged at 1240 K (1775°F) were subjected to 24-hour second-step aging treatments at 1035 K (1400°F), 1060 K (1450°F), 1090 K (1500°F), 1115 K (1550°F), 1145 K (1600°F), and 1170 K (1650°F).

Results for transverse 1255 K (1800°F)/21 MPa (3 KSI) creep tests are presented in Table 27. From these data, it would appear that the best creep properties for material solution treated at 1420 K (2100°F) are derived from a two-step aging treatment as follows: 1240 K (1775°F)/8 hours/AC + 1060 K (1450°F)/24 hours/AC. Compared with the results reported in Table 27 for the standard single-step age of 1170 K (1650°F)/4 hours/AC, this heat treatment yields a creep strength improvement of $\Delta P_K = 350$ to 365 ($\Delta P_R = 630$ to 660) Larson-Miller parameter units at temperatures near 1255 K (1800°F).

Table 26

Effect of Aging Treatment Upon the 1145 K (1600°F) Tensile Properties for Material Solution Treated at 1420 K (2100°F)/30 Minutes/AC

Aging Treatment	U.T.S.		0.2% Y.S.		El.
	(MPa)	(KSI)	(MPa)	(KSI)	(%)
1170 K (1650°F)/4 Hours/AC	745	108	625	91	7
	725	105	580	84	8
	740	107	565	82	10
	715	104	530	77	13
	670	97	510	74	10
1225 K (1750°F)/8 Hours/AC	730	106	435	63	16
+ 1145 K (1600°F)/24	705	102	415	60	12
Hours/AC	705	102	450	65	14
1240 K (1775°F)/8 Hours/AC	780	113	470	68	15
+ 1145 K (1600°F)/24	670	97	455	66	17
Hours/AC					

74

Table 27

Effect of Final Aging Treatment Upon the Creep Properties of Material Solution Treated at 1420 K (2100°F)/30 Minutes/AC and Intermediate Aged at 1240 K (1775°F)/8 Hours/AC

Final Aging Treatment		Hours to Percent Creep at 1255 K/21 MPa (1800°F)/3 KSI)	
		0.5%	1.0%
1035 K (1400°F)/24 Hours/AC		111	213
		238	483
	log Av.*	163	321
1060 K (1450°F)/24 Hours/AC		153	264
		310	555
	log Av.	218	383
1090 K (1500°F)/24 Hours/AC		123	209
		89	169
	log Av.	105	188
1115 K (1550°F)/24 Hours/AC		131	248
		113	204
	log Av.	122	225
1145 K (1600°F)/24 Hours/AC		212	450
		153	263
		146	242
		100	170
	log Av.	148	264
1170 K (1650°F)/24 Hours/AC		111	200
		127	227
	log Av.	119	213
1170 K (1650°F)/4 Hours/AC**		125	220
		104	174
	log Av.	114	196

* Antilog of the average of the logarithms of the test hours.
** No intermediate age.

4.0 CRYSTALLOGRAPHIC TEXTURE STUDY

The development of a crystallographic sheet texture represents a possible means of improving creep strength. Barrett et al. (ref. 23-24) investigated the effect of the cube texture on creep strength in copper. The sheet material was produced by cold reducing 97 percent and recrystallizing to give an average grain diameter of 0.03 mm (ASTM 7). The steady state creep rates of the textured sheet was found to be about half that for random polycrystals and independent of tensile axis orientation. The beneficial effects of the cube texture were interpreted in terms of the low angle boundaries ($\sim 5°$ average misorientation angle) serving as poor vacancy sources for dislocation climb.

In a more recent study, Klarstrom (ref. 25) investigated the effect of crystallographic texture on the low strain (≤ 1 percent) creep strength of HAYNES® alloy No. 188 thin gauge sheet. Significant improvements in low strain creep strength were obtained in sheets given 80 percent cold work followed by an anneal at 1505 K (2250°F). The major components of the texture were identified as (110) [$\bar{1}$10] and (112) [$\bar{1}$10]. The creep strength of the textured sheets was observed to be superior to that of standard production sheets in the 920 K (1200°F) to 1255 K (1800°F) temperature range.

In the present study, the possibility for improving the low strain creep strength of alloy No. R-41 through generation of a preferred crystallographic annealing texture was evaluated. Samples of 4.75 mm (0.187-inch) thick hot-rolled plate were cold rolled to 0.64 mm (0.025-inch) thick sheet employing levels of final reduction between 40 percent and 80 percent following the last intermediate anneal. These materials were then subjected to final solution treatments at 1310 K (1900°F), 1365 K (2000°F), and 1420 K (2100°F).

Following solution treatment, each of the materials was examined for the presence of preferred crystallographic texture in the plane of the sheet using the diffractometer reflection method. Samples were first sheared into approximately 25.4 mm (1-inch) squares, and the surface of each specimen was prepared by hand polishing on 220 grit through 600 grit silicon carbide papers then electropolishing for 15 seconds in a solution composed of 10 percent H_2SO_4–90 percent methanol. The prepared sample was then placed in a Philips-Norelco pole figure device and exposed to CoK_α radiation. During exposure, the device tilted and rotated the sample about the x-ray beam such that the resultant motion described a spiral in the plane of the stereographic projection. The maximum angle of tilt was limited to 55 degrees due to absorption of the beam by the sample.

The diffracted x-ray intensities were monitored by a solid state scintillation counter and recorded on a strip chart. Integrated intensities were also determined at 12-second intervals and recorded on

---

® HAYNES is a registered trademark of Cabot Corporation.

paper tape. Upon completion of the x-ray scan, the integrated intensities were read into a computer for analysis. The computer program employed (ref. 26) corrected the data for absorption, converted the corrected data into relative intensities, and printed out the results in a rectangular array which placed each value in its correct angular location on the stereographic projection. These intensity values were then normalized to an average random level, and boundaries were drawn between the areas representing measured intensities in terms of a multiple of the random intensity level.

Typical (111) pole figures for material given a cold rolling finish reduction of 40 percent and 80 percent with a 1420 K (2100°F) solution treatment are shown in Figures 31 and 32. All of the (111) pole figures for each reduction level were similar, regardless of solution treatment temperature. As may be observed from Figures 31 and 32, increasing the final cold rolling reduction from 40 percent to 80 percent did yield a change in the nature of the observed crystallographic texture; however, the strongest texture components at both levels of reduction had intensities less than three times random intensity. This is not indicative of a highly pronounced texture development.

Screening of transverse creep properties for several of the materials produced was performed using the specimen configuration shown in Appendix A and test conditions of 1145 K (1600°F)/97 MPa (14 KSI). Results are shown in Table 28. These data indicate clearly that any and all increase in properties observed in this study could be attributed to coincident grain size effects rather than any strengthening as a result of the development of any preferred crystallographic texture.

R.D.

T.D.

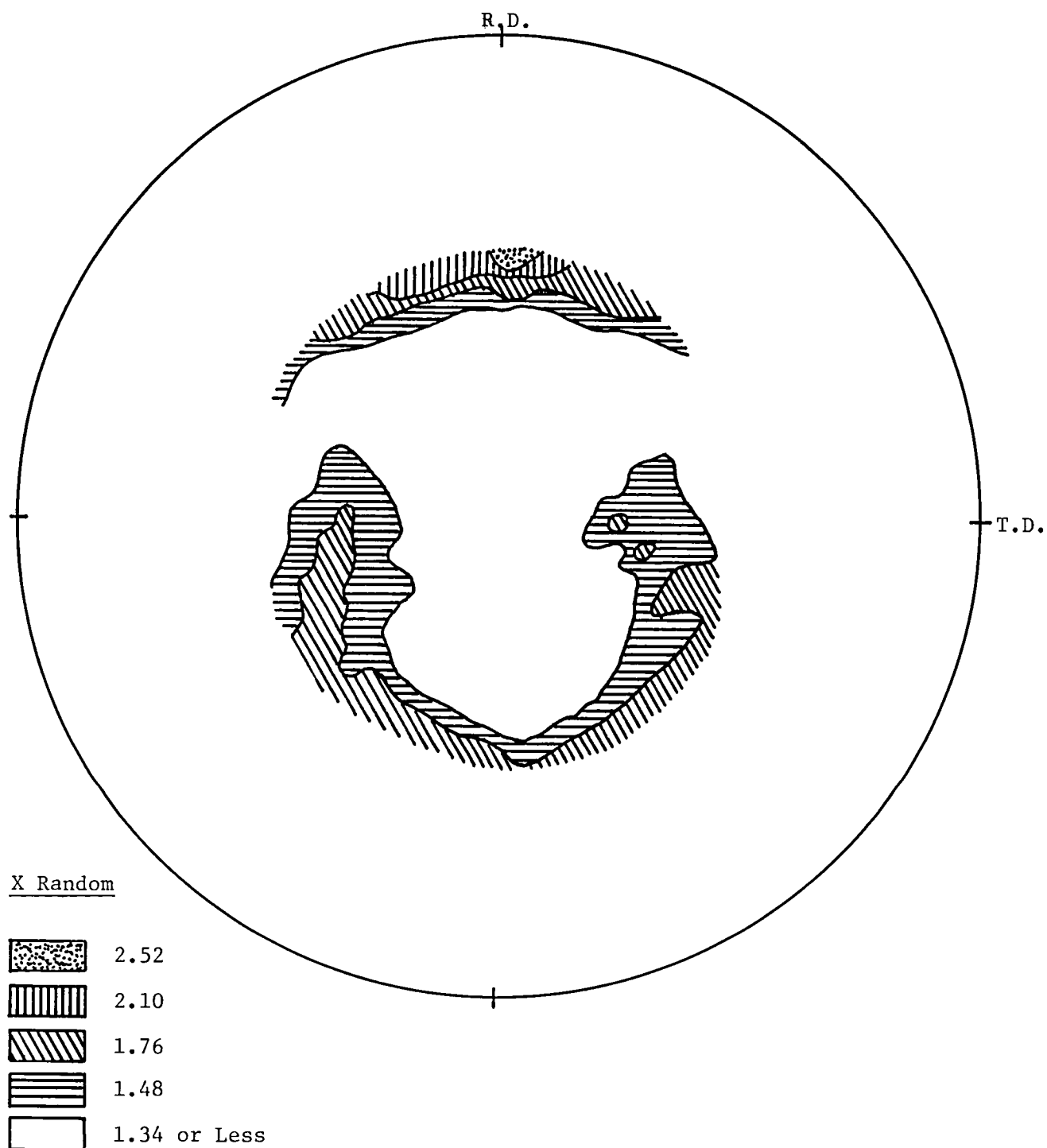X Random

2.52

2.10

1.76

1.48

1.34 or Less

Figure 31: (111) pole figure for material annealed at 1420 K
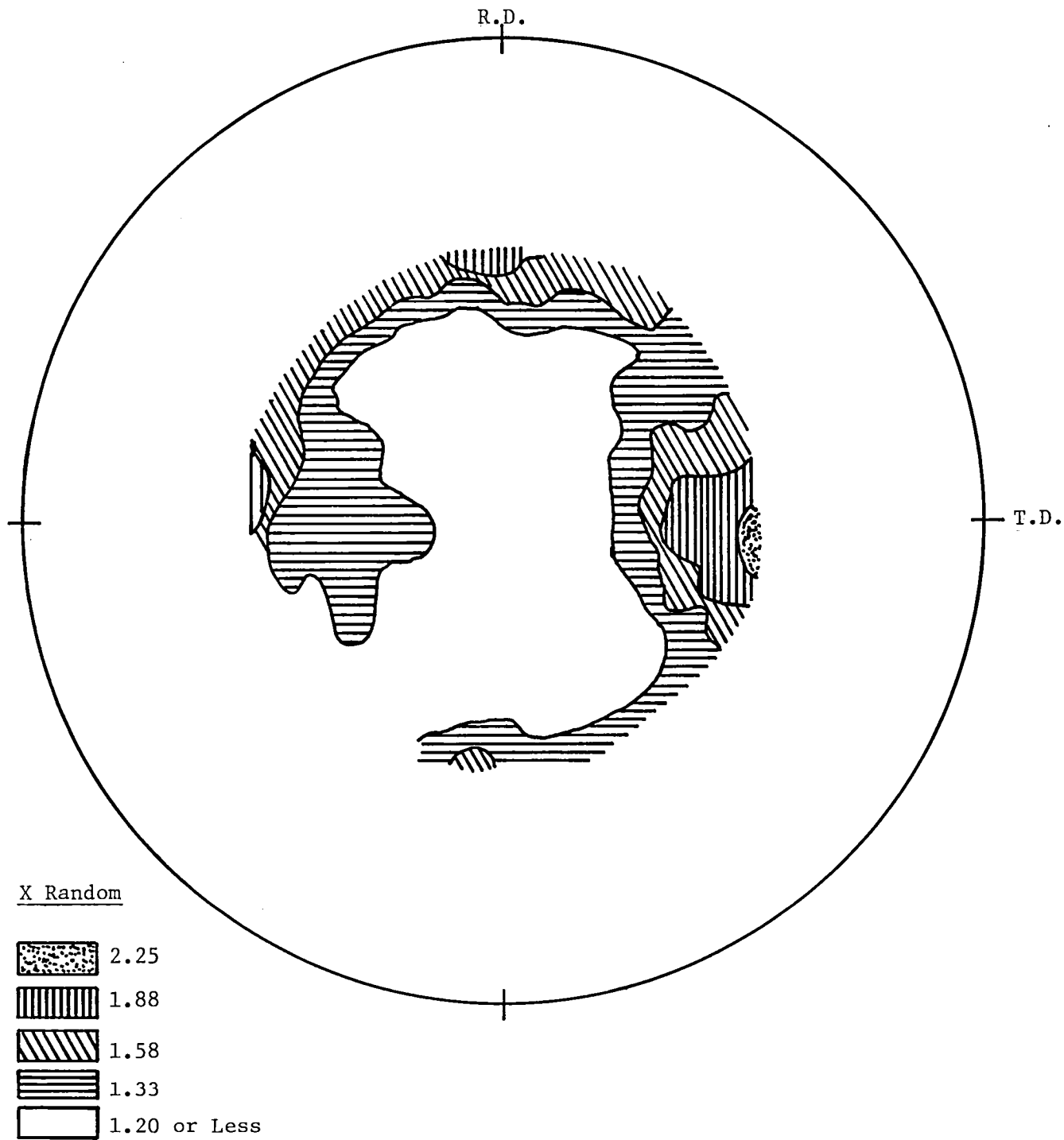(2100°F) after 40-percent cold work. (Central 55°
zone of pole figure shown, only.)

Figure 32: (111) pole figure for material annealed at 1420 K
(2100°F) after 80-percent cold work. (Central 55°
zone of pole figure shown, only.)

Table 28

Summary of Crystallographic Texture Study Creep Test Data

Percent Final (Cold Work)	Solution Treatment Temperature*	ASTM Grain Size	Hours to Percent Creep at 1145 K/97 MPa (1600°F/14 KSI)	
			0.5%	1.0%
30% (Baseline)	1395 K (2050°F)	6-7	56	116
			61	127
			78	154
		log Av.**	64	131
40%	1365 K (2000°F)	6-7	49	96
			52	100
			64	124
		log Av.	55	106
80%	1365 K (2000°F)	6-7	59	113
			68	133
			73	141
		log Av.	66	128
30% (Baseline)	1420 K (2100°F)	4-5	98	251
			112	307
			126	284
		log Av.	111	280
40%	1420 K (2100°F)	4-5	89	207
			92	232
			111	272
		log Av.	97	236
80%	1420 K (2100°F)	4-5	109	253
			138	280
			140	309
		log Av.	128	280

* All samples aged at 1170 K/4 hours after 30-minute solution treatment.

** Antilog of the average of the logarithms of the hours.

5.0 DISCUSSION AND CONCLUDING REMARKS

The primary objective of the program was to obtain improvements in the low strain ($\leq$ 1 percent) creep strength of CABOT alloy No. R-41 thin gauge sheet product by means of improved thermomechanical processing treatment. Two major approaches to achieving this objective were undertaken. One was to examine the development of an optimized heat treatment to provide a coarse grain structure without concomitant adverse effects upon tensile properties. The other was to determine if low strain creep properties could be improved by developing a preferred crystallographic orientation in the cold-rolled and annealed sheet.

Of these two approaches, only the heat treatment development yielded successful results. Efforts to produce a strong crystallographic annealing texture in alloy R-41 sheet by employing prior cold-rolling reductions of up to 80 percent were unsuccessful, and no creep strength advantage was derived. The two heat treatments developed, however, both provided for significant increases in 0.5 percent and 1.0 percent creep strength.

The more ambitious of the two new heat treatments consists of solution treating the material at 1475 K (2200°F)/30 minutes, furnace cooling at approximately 55 K (100°F) per hour to the first aging temperature of 1225 K (1750°F)/4 hours/air cool, plus a second age at 1090 K (1500°F)/24 hours/air cool. This heat treatment provides for a substantial increase in average low strain creep strength, as measured by an upward shift in a plot of strength versus the Larson-Miller parameter of as much as ΔP_K = 1,100 (ΔP_R = 2,000) parameter units in the vicinity of 1255 K (1800°F). This advantage decreases gradually with decreasing temperature, and at temperatures below about 1090 K (1500°F), the new heat treatment is less effective than the standard baseline heat treatment.

The improved creep properties developed with this new heat treatment are accompanied by tensile ductility for temperatures at or above 1035 K (1400°F), which is equivalent to or better than that produced with the standard baseline heat treatment. At temperatures below 1035 K (1400°F), the tensile ductility is reduced, but to still acceptable levels for this class of material. Of lesser importance, yield strength obtained with the new heat treatment is reduced relative to that of baseline heat-treated material.

The second, less ambitious of the two new heat treatments consists of solution treating the material at 1420 K (2100°F)/30 minutes/AC and aging the material in two steps--1240 K (1775°F)/8 hours/AC plus 1060 K (1450°F)/24 hours/AC. This heat treatment provides for a smaller increase in creep strength than that produced by the higher solution treatment temperature approach, but tensile properties do not appear to be significantly affected. The shift in the creep strength of the material in terms of the Larson-Miller parameter is about ΔP_K = 350 to 365 (ΔP_R = 630 to 660) parameter units at temperatures near 1255 K (1800°F). The advantage or disadvantage at lower temperatures was not determined.

A final comment must be made regarding properties. The evaluations described did not include many properties relevant to high-temperature applications such as weldability and weld strength efficiency, formability, property response to forming and annealing operations, isothermal low cycle fatigue, and thermal stability, to mention a few. These areas will have to be investigated if materials given the developed heat treatments are to receive serious design consideration.

APPENDIX A

CREEP TESTING PROCEDURE

All creep tests were carried out in air. The specimen configuration employed is shown in Figure A-1. To prevent distortion around the pinning holes, tabs were spot welded to the grip ends of each sample. A rigid frame extensometer was fastened to the specimen in the reduced test section as illustrated in Figure A-2. The knife edges of the extensometer were spaced 50.8 mm (2-inches) apart.

Two thermocouples were wired to the sample test section. One was used to control the furnace temperature, while the other was used to obtain an independent check of specimen temperature. Throughout each test, the temperature was maintained to within ± 1.7 K ($\pm 3°F$) of the required temperature. Before the test load was applied, the assembly was allowed to soak at temperature for at least 30 minutes.

Creep deformation, exclusive of the instantaneous loading strain, was measured using a single linear variable differential transformer (LVDT). The resolution of the LVDT measuring system was 2.54×10^{-4} mm (1×10^{-5} in.). The test data were electronically stored and read out after test by a computer. Tests were discontinued after a creep strain greater than 1% had been reached.
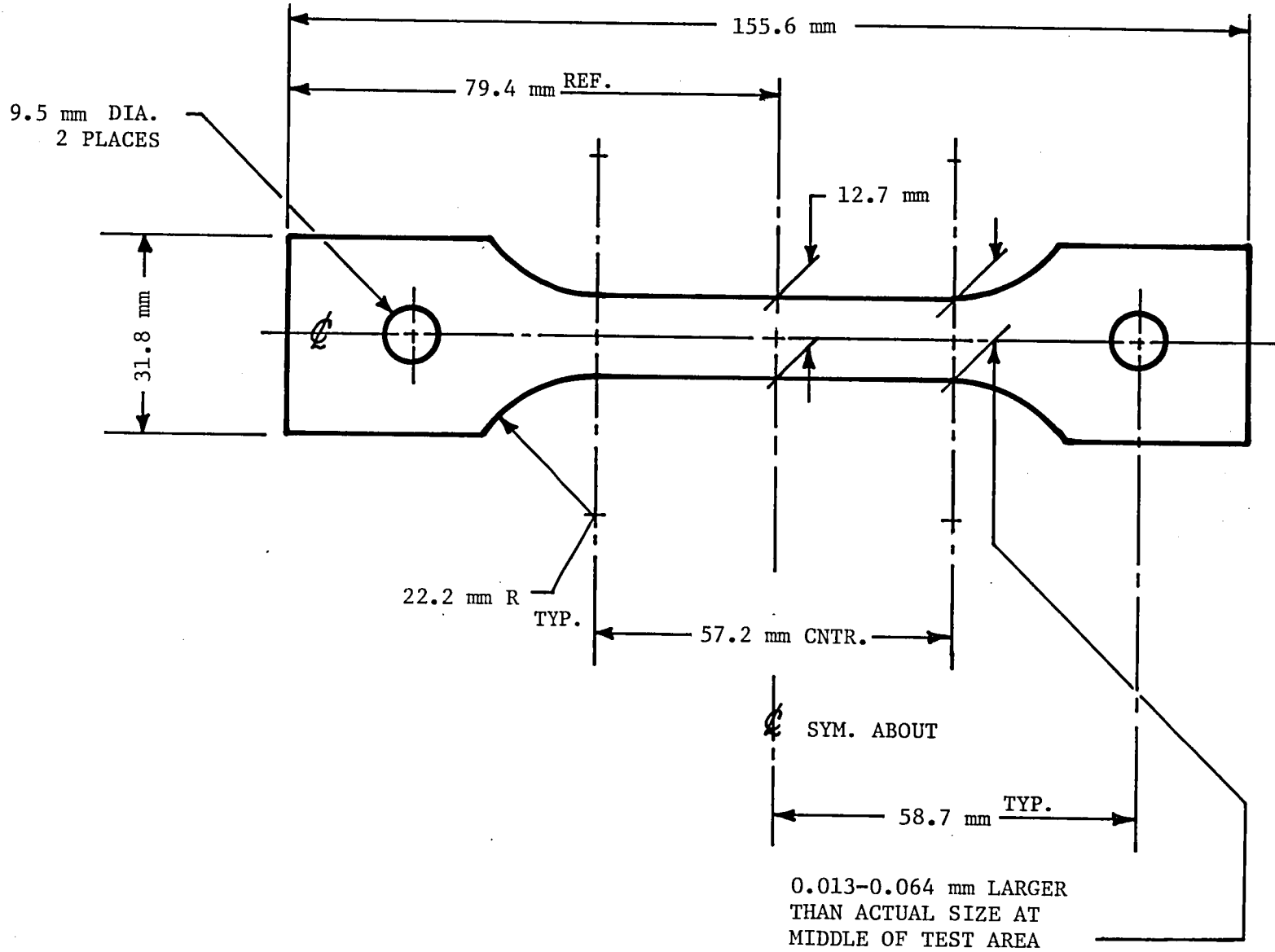
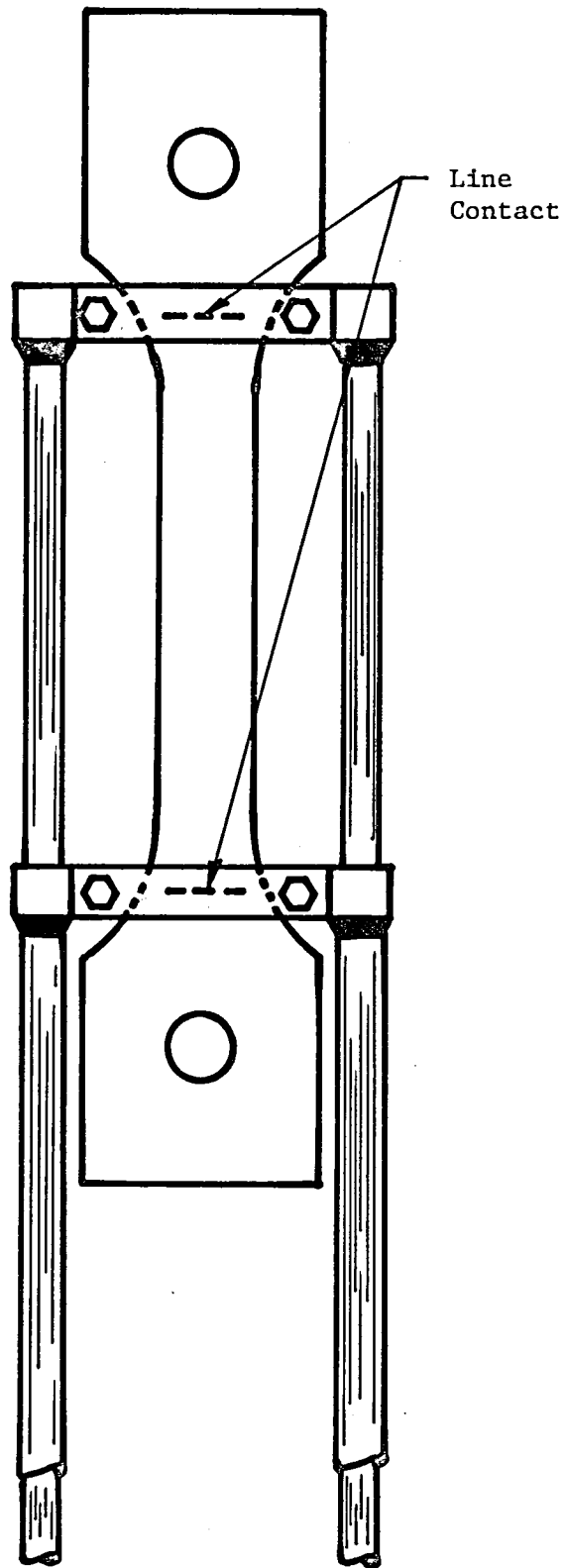Figure A-1: Creep and Tensile Test Specimen Configuration.

Line
Contact

Figure A-2: Creep Extensometer System   85

REFERENCES

1. Davis, J. W.; and Cramer, B. A.: Prediction and Verification of Creep Behavior in Metallic Materials and Components for the Space Shuttle Thermal Protection System - Phase I - Cyclic Materials Creep Predictions. NASA CR-132605-1, 1974.

2. Greene, A.; Sieber, H.; Wells, D.; and Wolfe, T.: Research Investigation to Determine Mechanical Properties of Nickel- and Cobalt-Base Alloys for Inclusion in Military Handbook-5, Volume I. AFML, Air Force Systems Command ML-TDR-64-116, 1964.

3. McBride, J. G.; Mulhern, B.; and Widmer, R.: Creep-Rupture Properties of Six Elevated Temperature Alloys. ASD, Air Force Systems Command, WADD-TR-61-199, 1962.

4. Kay, R. C.; and Chambers, J. W.: Tensile and Creep Properties of 0.010- and 0.050-Inch René 41 Alloy Sheet from Room Temperature to 2000°F. PR281-1Q-1, The Marquardt Corp., Van Nuys, California, 1962.

5. Hess, R. D.: High-Temperature Properties of HAYNES Wrought Alloys, Creep Data for 0.05-Inch HAYNES alloy No. R-41. No. 5546, Cabot Corporation, Kokomo, Indiana, 1961.

6. General Electric Company Material Specification No. B50TF76-S4, December 7, 1972.

7. Conway, J. B.; Stress Rupture Parameters: Origin, Calculation and Use. Gordon and Breach Science Publishers, Inc., 1969, pp. 21-84.

8. Decker, R. F.; and Sims, C. T.: The Metallurgy of Nickel-Base Alloys. The Superalloys, C. T. Sims and W. C. Hagel, eds., John Wiley and Sons, 1972, pp. 33-78.

9. Chang, W. H.: Basic Cause of Cracking in René-41 Sheet Alloy. DM58302 (58AD-16), General Electric Company, Cincinnati, Ohio, 1958.

10. Hall, A. M.; and Beuhring, V. F.: Thermal and Mechanical Treatments for Nickel and Some Nickel-Base Alloys: Effects on Mechanical Properties. NASA SP-5106, 1972.

11. Prager, M.: Study of Heat Treatments for Assuring Satisfactory Ductility in René 41. MPR No. 6-176A-839, Rocketdyne Division of North American Aviation, Canoga, California, 1966.

12. Slunder, C. J.; and Hall, A. M.: Thermal and Mechanical Treatments for Nickel and Selected Nickel-Base Alloys and Their Effects on Mechanical Properties. NASA TMX-53443, 1966.

13. Moon, D. P.; Barker, J. F.; and Simmons, W. F.: High-Temperature Properties of René 41 and Astroloy. Metals Engineering Quarterly, Vol. 1, February, 1961, pp. 3-11.

14. Kossowsky, R.; and Moon, D. P.: Effect of Thermo-Mechanical-Pressure Variables on Precipitation in René 41. Transactions of the Japan Institute of Metals, Vol. 9, 1968, pp. 398-405.

15. Weisenberg, L. A.; and Morris, R. J.: How to Fabricate René 41. Metals Progress, Vol. 78, No. 5, 1960, pp. 70-74.

16. Decker, R. F.; Rowe, J. P.; Bigelow, W. C.; and Freeman, J. W.: Influence of Heat Treatment on Microstructure and High-Temperature Properties of a Nickel-Base Precipitation-Hardening Alloy. NACA TN 4329, 1958.

17. Kaufman, M.: Control of Phases and Mechanical Properties in Nickel-Base Alloys of the René 41 Type. Trans. of the TMS-AIME, Vol. 227, April, 1963, pp. 405-422.

18. Murphy, H. J.; Sims, C. T.; and Heckman, G. R.: Long-Time Structures and Properties of Three High-Strength, Nickel-Base Alloys. Trans. of the TMS-AIME, Vol. 239, December, 1967, pp. 1961-1978.

19. Lacy, C. C.; and Albertin, L.: How to Heat Treat Space Age Materials. Metals Progress, Vol. 81, No. 3, 1963, pp. 89-95.

20. Loomis, W. T.; Freeman, J. W.; and Sponsellar, D. L.: The Influence of Molybdenum on the Gamma Prime Phase in Experimental Nickel-Base Superalloys. Metallurgical Transactions, Vol. 3, No. 4, 1972, pp. 989-1000.

21. Gluck, J. V.; and Freeman, J. W.: Effect of Creep Exposure on Mechanical Properties of René 41. Air Force Systems Command, ASD TR 61-73, 1961.

22. Popp, H. G.: Materials Property Data Compilation, Part I: René 41 Sheet and Strip. AF33(657)-8017, General Electric Company, Cincinnati, Ohio, 1962.

23. Barrett, C. R.: The Influence of Grain Boundaries and Stacking Faults on High-Temperature Plastic Deformation. Third Technical Report, N-ONR-225(60), NR-031-682, 1964.

24. Barrett, C. R.; Lytton, J. L.; Sherby, O. D.: Effect of Grain Size and Annealing Treatment on Steady State Creep of Copper. Transactions of TMS-AIME, Vol. 239, No. 2, 1967, pp. 170-180.

25. Klarstrom, D. L.: Thermomechanical Processing of HAYNES alloy No. 188 Sheet to Improve Creep Strength. NASA CR-3013, 1978.

26. Klappholy, J. J.; Waxman, S.; and Feng, C.: A Computerized Technique of Plotting a Complete Pole Figure by an X-ray Reflection Method. Advances in X-ray Analysis, Vol. 15, Plenum Press, 1972, pp. 365-372.

1. Report No. NASA CR-172392	2. Government Accession No.	3. Recipient's Catalog No.
4. Title and Subtitle Development of Improved Low-Strain Creep Strength in CABOT® alloy R-41 Sheet		5. Report Date August 1984
		6. Performing Organization Code
7. Author(s) Michael F. Rothman		8. Performing Organization Report No. 11816
		10. Work Unit No.
9. Performing Organization Name and Address Cabot Corporation 1020 W. Park Avenue Kokomo, IN 46901		11. Contract or Grant No. NAS1-15975
		13. Type of Report and Period Covered Contractor Report
12. Sponsoring Agency Name and Address National Aeronautics and Space Administration Washington, DC 20546		14. Sponsoring Agency Code

15. Supplementary Notes

Langley Technical Monitor: Donald R. Rummler
Final Report

16. Abstract An investigation was undertaken to determine if the low-strain creep properties of CABOT® alloy No. R-41 thin gauge sheet could be improved through modified heat treatment or through development of a preferred crystallographic texture. The application for such an optimized form of material would be in the construction of heat shields for advanced reentry vehicles such as the space shuttle. The basic approach taken to improve the creep strength of the material by heat treatment was to increase grain size by raising the solution treatment temperature for the alloy to the range of 1420 K to 1475 K (2100°F to 2200°F). It was recognized that the key technical issue involved in this approach was maintenance of adequate tensile ductility following the solutioning of M_6C primary carbides during the higher temperature solution treatment. The approach to improving creep properties by developing a sheet texture involved varying both annealing temperatures and the amount of prior cold work.

As a result of these studies, a new heat treatment was identified for alloy R-41 sheet which yields a substantial creep-life advantage at temperatures above 1090 K (1500°F) when compared with material given the standard heat treatment. At the same time, the new treatment provides reasonable tensile ductility over the entire temperature range of interest. A detailed compari- son of the mechanical properties of the material given the new heat treatment with those for material given the standard heat treatment is presented. Attempts to improve creep strength by developing a sheet texture were unsuccessful.

17. Key Words (Suggested by Author(s)) alloy R-4 thin sheet creep properties heat treatment crystallographic texture	18. Distribution Statement Unclassified-Unlimited

19. Security Classif. (of this report) Unclassified	20. Security Classif. (of this page) Unclassified	21. No. of Pages 87	22. Price